Spring 5-7-2016

Mechanisms of lateral-inhibitory feedback from horizontal cells to cone photoreceptors at the first synapse of the retina

Ted J. Warren
University of Nebraska Medical Center

Mechanisms of lateral-inhibitory feedback from horizontal cells to cone photoreceptors at the first synapse of the retina

by

Ted John Warren

A DISSERTATION

Presented to the Faculty of

the University of Nebraska Graduate College

in Partial Fulfillment of the Requirements

for the Degree of Doctor of Philosophy

Pharmacology & Experimental Neuroscience Graduate Program

Under the Supervision of Professor Wallace B. Thoreson

University of Nebraska Medical Center

Omaha, NE

January, 2016

Supervisory Committee:

Wallace B. Thoreson, Ph.D.	Jyothi Arikkath, Ph.D.
George Rozanski, Ph.D.	Gary Pickard, Ph.D.

This work is dedicated to my children, Lola and Kelvin Warren.

Acknowledgements

I would like to thank my mentor Dr. Wallace (Wally) B. Thoreson for his tutelage and support throughout this project. Wally guided, discussed, critiqued, and sometimes physically helped me throughout this project by not only through dialoguing about and planning, but by also performing experiments with or alongside of me. Wally was always supportive and served as a model for how to manage a productive lab, which I will carry with me through the rest of my career. My mother and I believe that Wally's example for me went beyond the laboratory, and made me that much better of a dad. I would also like to thank my dissertation committee: Dr. Jyothi Arikkath, Dr. George J. Rozanski, and Dr. Gary Pickard for their advice and support of my thesis project.

I would also like to thank all the laboratory members who not only contributed in some shape or form to this work, but also the individual friendships I developed with them. In particular, I would like to thank Dr. Matthew (Matt) J. Van Hook for serving as a mentor and fellow-admirer of the patch-clamping technique. Matt helped with and performed experiments, discussion, editing, and is responsible for my development as a scientist through critiquing and granting unlimited access to his library. I would also like to thank Dr. Minghui Chen, Dr. Karlene Cork, Xiangyi Wen, Justin Grassmeyer, Jennie P. Smith, Sylvie Sim, for the discussions and support in helping to obtain my Ph.D.

I would like to thank staff members within the departments of Ophthalmology & Visual Sciences and Pharmacology & Experimental Neurosciences, particularly Theresa Grutel, Sandra Mahoney, Robin Taylor, Leticia Tran, Jill Daley, and Susan Davis for their secretarial assistance along with arranging trips for research purposes. Finally, I would like to acknowledge and thank Dr. Myron Toews and Dr. Keshore Bidasee for all their time and work with the graduate students of the PEN, including myself. I hope they realize their time and efforts do not go unnoticed.

Finally, I want to thank my parents, Kathy and Kirby Warren for their support, both emotional and physical. Grandma Kathy was always willing to watch and spend time with the kids when I needed more time to write or do an experiment. Both grandparents have contributed to both kids development as wonderful individuals. And to my children, Lola Renee and Kelvin Eli, with whom I hope that this work continues to build us a brighter future.

Table of Contents

List of Figures

Introduction

Results

MECHANISMS OF LATERAL-INHIBITORY FEEDBACK FROM HORIZONTAL CELLS TO CONE PHOTORECEPTORS AT THE FIRST SYNAPSE OF THE RETINA

Ted J. Warren, Ph.D.

University of Nebraska, 2016

Supervisor: Wallace B. Thoreson, Ph.D.

Polarization of the horizontal cell (HC) membrane potential causes changes in the synaptic cleft pH that result in inhibitory feedback from HCs to cone photoreceptors (PRs). HCs average signals from many PRs and so negative feedback onto PR terminals from HCs subtracts the average luminance of the visual scene from the light responses of an individual cone. This feedback operates by changing the voltage-dependence and amplitude of the L-type Ca^{2+} current (I_{Ca}) that regulates synaptic release. Feedback regulation of PR Ca^{2+} channels involves protons but the mechanism by which this pH change occurs is unclear. We investigated three possible sources for protons in the cone synaptic cleft: 1) extracellular carbonic anhydrase (CA), 2) protons released into the cleft upon exocytosis of synaptic vesicles, and 3) sodium-hydrogen exchangers (NHEs). Using electrophysiological measurements of HC to cone feedback, we found that CA and vesicular protons are not major sources of protons for feedback. Feedback was eliminated by removal of extracellular Na^{+} and significantly inhibited by an NHE antagonist, cariporide, implicating NHEs as a significant source of protons. While NHEs are a major proton source, they are not known to be voltage-sensitive and thus unlikely to be responsible for changes in extracellular proton levels caused by changes in HC membrane potential. Instead we found that removal of bicarbonate and inhibition of bicarbonate transporters with 500 μM DIDS both eliminated feedback, suggesting that HC polarization changes extracellular pH by altering bicarbonate transport.

To test whether an ephaptic mechanism is involved in mediating feedback, we

used paired whole cell recordings to hyperpolarize the HC while cone I_{Ca} was active and then measured the kinetics of feedback-induced changes in the cone membrane current. The time constants of the resulting feedback current were slower than the measurement time resolution and not instantaneous as predicted by an ephaptic mechanism.

"It is a capital mistake to theorize before one has data. Insensibly one begins to twist facts to suit theories, instead of theories to suit facts."

Sherlock Holmes

-A Scandal in Bohemia

Chapter 1

1.1 Anatomy of the retina

At the first synapse in the retina, visual information obtained by the cone photoreceptors (PRs) is encoded and transmitted to two types of downstream neurons: horizontal cells (HCs) and bipolar cells (BP cells). As we consider in this thesis, the information transmitted by photoreceptors is shaped by an iconic neural circuit: a lateral-inhibitory feedback circuit (Byrne & Roberts, 2009). Lateral inhibition is defined as the activity of one neuron having an inhibitory effect on its neighboring neurons (as opposed to those neurons that are downstream). The spatially extensive dendritic arbors of HCs receive synaptic inputs from many PRs but at the same time feed inhibitory signals back to PRs which modifies their synaptic output. Before turning to lateral-inhibitory feedback and why it is important in visual processing, I begin with a general review of the anatomy of the retina and the phototransduction mechanism employed by photoreceptors.

The retina is a thin piece of neuronal tissue (~200 μm in depth) that lines the back of the eye. One advantage to studying the retina is that its cellular composition is well defined and it is easily accessible for examination as a tissue (Dowling, 2012). It is composed of five-principle types of neurons: PRs, HCs, BP cells, amacrine cells, and retinal ganglion cells (RGCs).

BP cells receive inputs from PRs and transmit them to third-order amacrine cells and RGCs. Information about the visual scene is separated into a dozen different parallel pathways created by a dozen different BP cell types (Masland 2012, see Euler *et*

al., 2014 for specific review of BP cells). These BP cells differ in their synaptic connections and response properties as a result of distinct anatomical and molecular features that involve differences in dendritic anatomy, glutamate receptors, and ion channels (Thoreson & Witkovsky, 1999; DeVries, 2000; DeVries *et al*., 2006; Puthussery *et al*. 2013).

HCs and amacrine cells are inhibitory interneurons although there exists a class of amacrine cells that release glutamate as a neurotransmitter (Lee *et al*., 2014). As discussed in greater detail later, there are 1-3 types of HCs in most retinas contacting PR terminals and BP cell dendrites. Amacrine cells send out their dendritic projections laterally to contact BP cell terminals, other amacrine cells, and RGCs. There are at least 29 amacrine cell types (Masland, 2012). There are more than a dozen types of RGCs, maintaining the parallel processing of visual information into multiple different functional streams initiated by BP cells (Masland, 2012).

While most of the light-evoked signals that reach the brain originate with the responses of rods and cones, it has been recently recognized that some RGCs are intrinsically capable of responding to light without receiving upstream signals from cone or rod photoreceptors. These RGCs, known as intrinsically photosensitive retinal ganglion cells (ipRGCs) have been shown to be necessary for photoentrainment of the circadian rhythm, the pupillary light reflex, and sleep (Pickard & Sollars, 2011). Intrinsic photoresponses of ipRGCs can also impact visual perception (Schmidt et al., 2014) and participate in retrograde signaling by activating dopaminergic amacrine cells to release dopamine. Release of dopamine within the retina has a neuromodulatory effect on the neurons in the outer retina (Zhang *et al*., 2008; Zhang *et al*., 2012).

In addition to many types of neurons, the retina also contains three types of glial cells. Muller cells are radial glial cells that extend from the inner surface to the outer

limiting membrane separating the inner and outer segments of photoreceptors. Microglia are the resident immune cells within the retina. Astrocytes can be found in the nerve fiber layer at the inner surface of the retina.

A vertical section of the retina reveals that the cell types are organized in laminar fashion. (Fig. 1A, B). PRs lie at the back of the retina and so, after being refracted through the cornea and the lens, light must pass through the other layers of the retina before reaching the PRs. Just proximal to the cell bodies of the PRs is the outer plexiform layer (OPL) which contains the synapses between PRs, HCs and BP cells. The inner nuclear layer (INL) contains the cell bodies of BP cells, HCs, and amacrine cells. Both the ONL and the INL are named because in the vertical section of the retina the nuclear bodies of the neurons appear irregularly clustered together forming distinct anatomical landmarks. The INL is sandwiched between the OPL and inner plexiform layer (IPL) and the ONL is layered above the OPL but below the OS of the PRs. The synapses between amacrine cells, BP cells, and RGCs form the IPL. The cell bodies of RGCs form a layer at the inner surface of the retina and their nerve fibers lie atop these cell bodies.

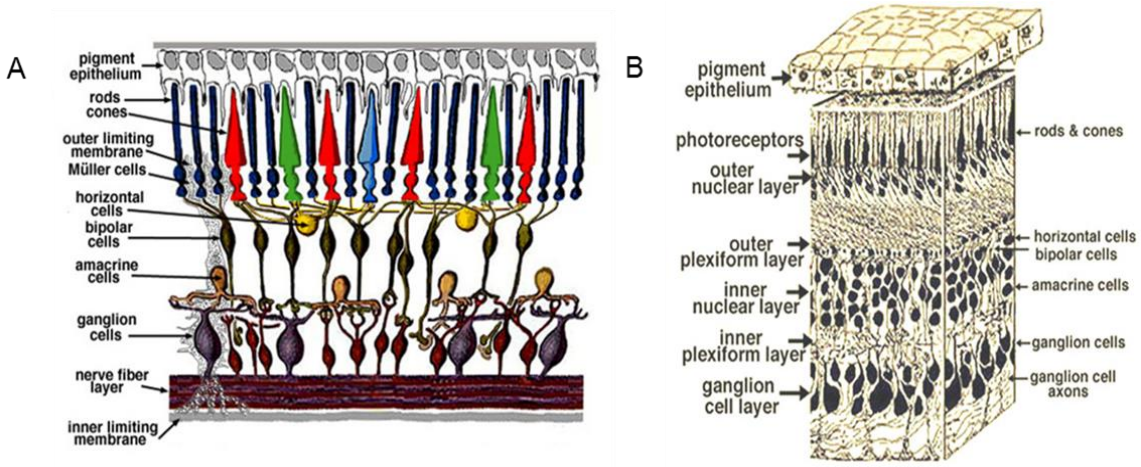

Figure 1. Cellular organization of the vertebrate retina. A) A cross-sectional diagram showing the major cell types of the retina. B) Three dimensional representation showing the cell types and major layers of the retina. The photoreceptors (PRs) make up the outermost layer, where their cell bodies form an anatomically distinct, visual landmark known as the outer nuclear layer (ONL). The PRs project towards the inner eye and form synapses onto the dendrites of HCs and bipolar cells. This synaptic layer is referred to as outer plexiform layer (OPL), and is where HC dendrites contact PR terminals. Bipolar cells send their axons toward the inner eye and form synapses with amacrine and RGCs, thus forming the inner plexiform layer (IPL). The cell bodies of HCs, bipolar, and amacrine cells make up the inner nuclear layer (INL). The cell bodies of the RGCs and their axons compose the retinal ganglion cell layer. Image taken under a Creative Commons license from: “Simple anatomy of the retina” by Helga Kolb, www.webvision.med.utah.edu.

The present thesis is concerned with elucidating the synaptic mechanism by which HCs have an inhibitory influence on the release of glutamate from cone terminals. The rest of the anatomical discussion will be concerned with this particular synapse, hereafter referred to as the first synapse in the retina or the tri-partite synapse. Readers interested in learning more on the encoding and transformation of signals downstream from this synapse may consult the following references (Masland, 2012; Euler *et al*., 2014; Vaney *et al*., 2012; Field & Chichilinsky, 2007).

1.2 Cone Photoreceptor Anatomy & Physiology

Cone and rod PRs are sensory neurons that respond to light rays of varying wavelengths. Rod PRs are specialized for detecting dim light during nighttime or scotopic conditions, while cones are less sensitive to light and thus involved in detecting brighter light during daytime or photopic conditions. Cone and rod photoreceptors both possess an outer segment (OS) that contains the phototransduction apparatus (Fig. 2). In rods, many of the molecules involved in phototransduction are packed into discs of membrane that look much like red-blood cells without the concave center. Rod discs are stacked one-on-top of another and ensheathed by a lipid bilayer membrane that is

contiguous with the rest of the cell. In cone PRs, the discs are not separate organelles but formed by infoldings of the plasma membrane of the OS. The inner segment (IS) is composed of a mitochondria-rich region called the ellipsoid and a nucleus. The OS is connected to the IS through a thin cilium. This cilium allows changes in the membrane potential in the outer segment to spread from the light-sensitive OS to the IS and down to the synaptic terminal. Synaptic terminals in rods and many cones sit at the end of an axonal process extending from the base of the IS.

Intracellular recordings by Tomita (1965) provided the first direct evidence that PRs hyperpolarize in response to light. This was a surprising finding because invertebrate PRs were known to depolarize in response to light, thereby increasing the release of NT. Toyoda *et al*. (1969) showed that the input resistance of vertebrate PRs increases upon light stimulation, indicating that light causes ion channels to close. Baylor and Fettiplace (1977) carried out a series of elegant experiments demonstrating that graded changes in the membrane potential of cone PRs are both necessary and sufficient for producing a downstream visual signal. Similar to approaches used in our experiments, Baylor and Fettiplace took advantage of the fact that changes in membrane potentials can be dictated by the experimentalist by introducing current through an electrode that impales the cell. They obtained an intracellular recording from a cone PR while at the same time recording action potentials extracellularly from an On-type RGC that responds to light by increases in firing rate. To show that hyperpolarization of the cone PR was necessary for signaling of visual information, the two shined a light on the retina to activate the On RGC. In darkness, injecting current to hyperpolarize the cone PR mimicked the effect of light and stimulated activity in On RGCs. Conversely, depolarizing the cone PR by injection of current antagonized On RGC responses to light. These results showed that changes in the membrane potential of the cone PR are sufficient for signaling visual information to RGCs (Baylor &

Fettiplace, 1977; Baylor, 1987).

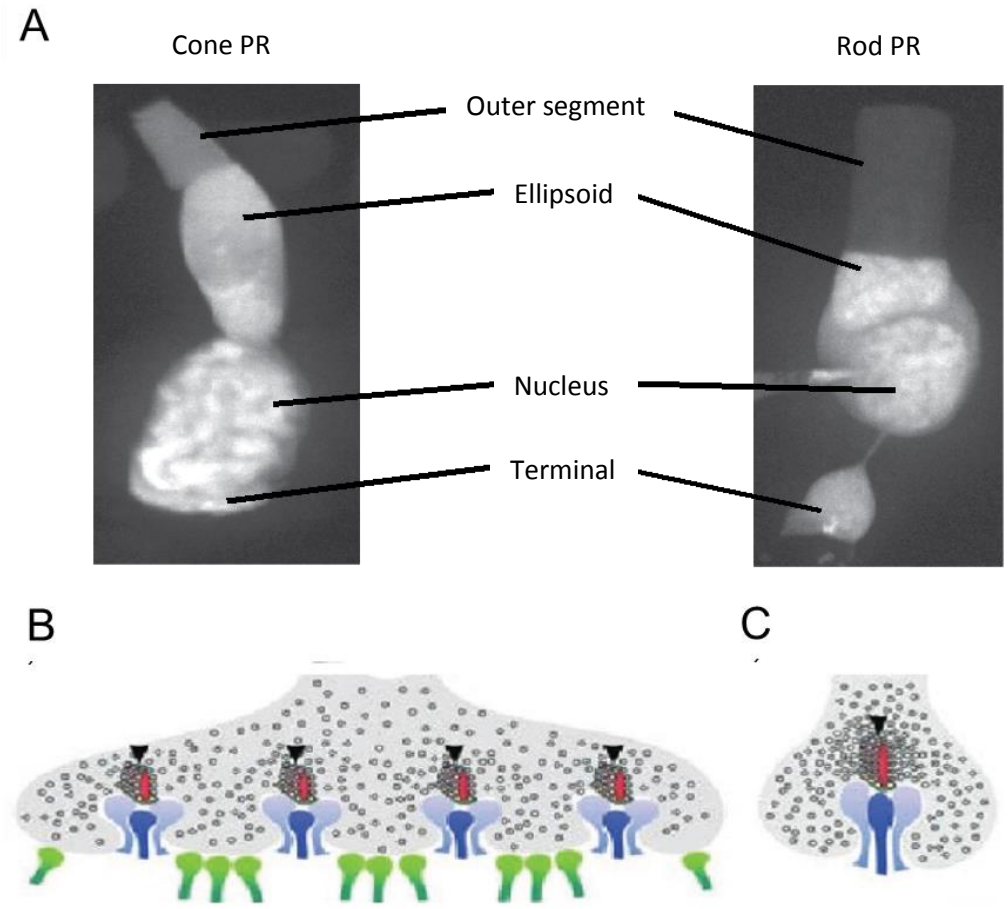

Figure 2. Anatomy of cone and rod photoreceptors (PRs). A) A cone and rod PR imaged in a vertical section of salamander retina. Cells were labeled with a calcium-sensitive dye, Oregon Green BAPTA 1. Rods and cones both have an outer segment (OS) that contain the light-sensitive opsin molecules. The inner segment (IS) contains the ellipsoid region which is filled with mitochondria. The nucleus is contained below, followed by the synaptic terminals. The cone synaptic terminal is termed the pedicle while the rod terminal is called the spherule. Images courtesy of Dr. Wallace B. Thoreson. **B-C)** Stylized representation of a cone pedicle (B) and rod spherule (C). Each cone pedicle contains multiple synaptic terminals with dendrites of HCs (light blue) and bipolar cells (darker blue) directly across from the cone's synaptic ribbons (black arrows). Ribbons tether glutamate-laden synaptic vesicles close to L-type Ca^{2+} channels. The green dendritic terminals represent flat basal contacts of Off-type bipolar cells. Image a) was taken with permission, under a Creative Commons license from: "Simple anatomy of the retina" by Helga Kolb, www.webvision.med.utah.edu. Images in b and c were taken with permission from Regus-Leidig & Brandstatter, Structure and function of a complex sensory synapse. *Acta Physiologica* (Oxford, England)(2012).

Most species have a single type of rod photoreceptor and multiple types of cones that differ from one another in their spectral sensitivities. The number of cone subtypes varies among species. The ability to compare responses from spectrally distinct cone types is required for color vision (Dowling, 2012). The different spectral sensitivities among cones arise from differences in the light-sensitive pigments they contain. This light-sensitive molecule, known as opsin, is contained within the photoreceptor OS (Masland, 2012). In Old World primates, cones contain opsins with spectral sensitivities that peak in either the long (red), middle (yellow/green), or short (blue) wavelengths. The experimental species used in our studies, salamander, possesses three morphologically distinct cone subtypes: small single cones, large single cones, and double cones. Double- and large single cones are sensitive to long wavelengths of light, while small single cones can be sensitive to UV-, red-, or blue-wavelengths of light (Sherry *et al*., 1998; Imamoto & Shichida, 2014). Collectively, cone PRs can respond to wavelengths of light between 360 – 780 nm.

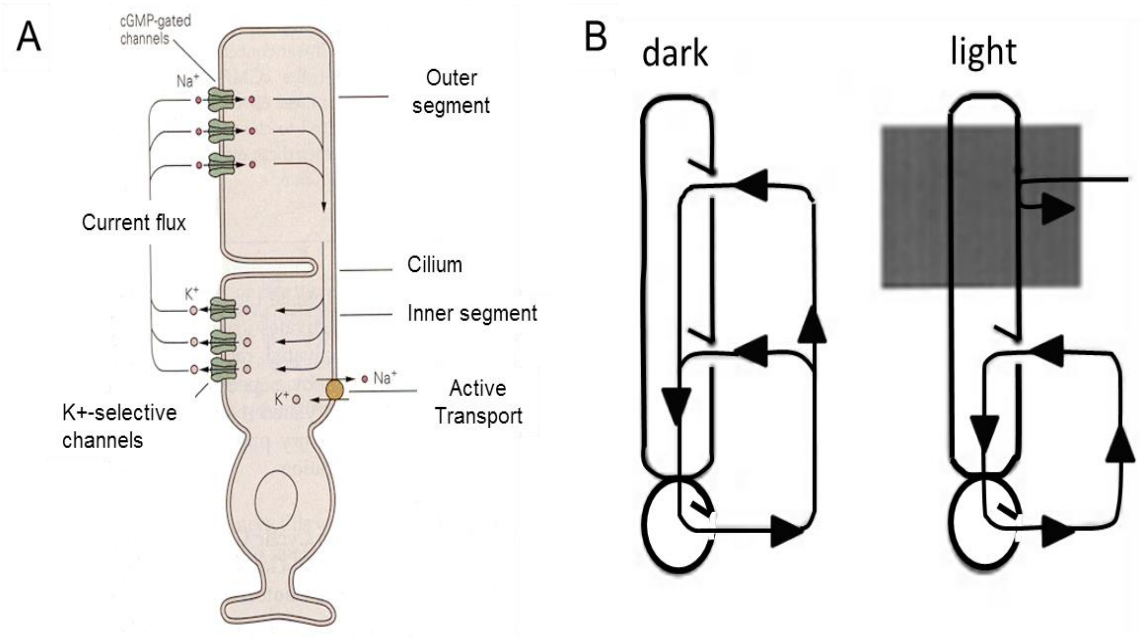

Figure 3. Generation of the dark current. A) Na^+ ions flow down their chemical gradient through cGMP-gated channels in the outer segment (OS) in the dark. The electrochemical driving force for K^+ drives these ions out through K^+-selective channels in the IS, thus completing the circuit. Na^+ ions are pumped out of the cell by Na^+/K^+-ATPases in the IS to maintain the low intracellular concentration of Na^+. **B)** Upon stimulation with light (represented by a large-grey box) the cGMP-gated channels close, part of the circuit is disconnected, and the amount of positive charge entering the cell decreases. There is still a strong-outwardly directed chemical force on K^+ ions and so the cell hyperpolarizes. Image **A)** is taken from Kandel, Schwartz, & Jessel. *Principles of Neuroscience*, 4th Ed. The McGraw-Hill Companies Inc., 2000. Image **B)** from Rieke & Baylor. Single-photon detection by rod cells of the retina. *Reviews of Modern Physics*.1998 July; 70(3):1027-36.

While cones are specialized for brighter light, rods are able to detect absorption of a single photon of light, as might occur when an individual is gazing at the stars on a clear, moonless night (Hecht *et al*., 1942; van der Velden, 1946; Rodieck, 1988). The greater sensitivity of rods extends the sensitivity of the visual system by roughly a thousand times.

Phototransduction is initiated when one of the opsin molecules in the OS catches a photon of light (Rodieck, 1998; Dowling, 2012). The opsin molecule in the rod OS is called rhodopsin whereas opsins in cones are typically referred to as cone opsins.

Opsins are transmembrane apoproteins (30-60 kD) with seven α-helices that surround a prosthetic group chromophore, 11-cis-retinal (11-cis-vitamin A aldehyde). An eighth helix runs parallel to the intracellular membrane and is involved in signaling to a G protein signaling pathway. 11-cis-retinal is covalently linked to a histidine residue within the seventh α-helix of the opsin. The chromophore forms a Schiff base with the opsin and the red shift induced by this protonation shifts the chromophore's absorption spectrum, allowing it to absorb wavelengths of light in the visible range from 360 to 600 nm. Variations within the amino acid sequence of different opsin subtypes alter their interactions with the chromophore and thus alter the absorption maxima. For example, differences in only three amino acid residues account for most of the 30 nm difference in peak spectral sensitivities of middle (M) and long (L) wavelength sensitive primate cones (Kawamura & Tachibanaki, 2014).

Upon absorption of a photon, the 11-cis-retinal moiety undergoes a cis-trans isomerization reaction and becomes 11-trans-retinal. This causes a conformational change in opsin and activates the opsin into a signaling state, where it interacts with a G protein known as Transducin (G_t). Each activated opsin moiety can interact with hundreds of G_t molecules, thus amplifying the signal. G_t, in its inactive conformation is a heterotrimeric protein composed of α-, β-, and γ-subunits. Absorption of photon by opsin causes G_t to exchange a molecule of GDP for GTP and G_t then disassociates into α- and βγ subunits. Upon dissociation, the active sites of the α- and βγ-subunits are exposed. The βγ complex is thought to be involved with the interaction of the opsin itself along with binding to deactivated α-subunits. It is not known to be involved directly in the transduction of the light signal itself. The Gα subunit then diffuses and eventually interacts with the membrane-anchored phosphodiesterase (PDE). PDE is involved in converting guanosine 3',5'-cyclic monophosphate (cyclic GMP) to guanosine

monophosphate (GMP). cGMP is a signaling molecule within the OS that diffuses freely and can bind to cyclic GMP-gated cation channels within the OS, thus opening the channels and allowing them to carry cations into the OS. Cyclic GMP-gated cation channels are permeable to Na^+, K^+ and Ca^{2+} ions. The net influx of Na^+, and to a lesser extent Ca^{2+}, causes the membrane to depolarize in darkness. Thus in darkness, photoreceptors have a membrane potential of approximately -35 to -45 mV (fig. 3). When PDE is activated it vigorously hydrolyzes cyclic GMP, reducing the molecule's concentration and the amount of binding of cyclic GMP to the cyclic GMP-gated cation channels. Closure of cGMP-gated channels reduces the inward cation current and thus hyperpolarizes the photoreceptor (Kawamura & Tachibanaki, 2014; Arshavsky *et al*., 2002; Luo *et al*., 2008). This change in membrane potential spreads throughout the cell, until it reaches the synaptic terminal where it affects the voltage-sensitive L-type Ca^{2+} channels.

Na^+ ions entering the cell through cation channels in the OS are extruded by Na^+/K^+ ATPases in the ellipsoid region of the IS. The activity of this pump is fueled by a dense accumulation of mitochondria at the outer margins of the IS (Wright, 2004). The continuous influx of Na^+ ions into the OS and extrusion of Na^+ ions out of the IS generates a circulating current in darkness (i.e., the "dark current") that passes from inner to outer segment in the extracellular space and through the cilium from outer to inner segment in the intracellular space (Fig. 3; Baylor, 1987).

1.3 Synaptic terminals of photoreceptors

The synaptic terminals of rods are typically found at the end of a thin axon. Rod terminals are called spherules for their characteristically spherical shape. In mammals, post-synaptic BP and HCs typically contact a rod terminal within a single invagination in

the spherule (Rao-Mirotznik *et al*., 1995; Migdale *et al*., 2003). The tips of the horizontal cells and BP cells within the invagination terminate adjacent to a plate-like protein structure within the rod terminal known as the synaptic ribbon. Synaptic ribbons are also found in cones and a variety of other sensory neuron synapses that tonically release NT, including hair cells, pineal photoreceptors, and retinal bipolar cells (LoGiudice & Matthews, 2009). Ribbons are involved in tethering, priming, and regulating the amount of the release of synaptic vesicles from the terminal region (Snellman *et al*., 2011; Jackman *et al*., 2009). The ribbon promotes synchronous release of vesicles, in that it tethers the vesicles and the exocytotic machinery within close proximity of the L-type Ca^{2+} channels, so that changes in V_m are more precisely coupled with changes in the amount of neurotransmitter released (Thoreson, 2007). The synapse between these three cell types--photoreceptors, HCs and BP cells--is known as a tripartite synapse.

Cone PRs have larger synaptic terminals called pedicles. Unlike rod spherules that exhibit a single invaginating synapse, cones contain many invaginations (Fig. 2B & C). In the primate retina, pedicles of foveal cones contains approximately 20 synaptic invaginations and peripheral cones can contain as many as 50 (Anhelt *et al*., 1990; Havercamp *et al*., 2001a). As shown in Fig. 4, HCs are lateral to the more central BP cell processes and extend deeper into the invagination. In mammals, On BP cell dendrites terminate directly across from the synaptic ribbon, whereas Off BP cells form basal contacts onto cone pedicles just outside of the invagination. Unlike this arrangement in mammals, in salamander retina about 80% of terminals have Off BP cells as their central elements and 80-90% of On BP cells form basal contacts outside of the terminal (Lasansky, 1973). In Fig. 4B, the long-vertical electron-dense structure is the synaptic ribbon. Cone ribbons are typically 0.2-1 μm long and 0.2-0.5 μm high (Pierantoni & McCann, 1981; Sterling & Matthews, 2005; Pang *et al*. 2008). Rod ribbons are larger,

extending 1-3 µm in length. Ribbons tether a large supply of vesicles near release sites. For example, individual rod PRs from the cat retina each possess approximately 3,600 vesicles (Schmitz, 2009). In salamander retina, each cone ribbon tethers ~100 vesicles and each rod ribbon tethers ~700 vesicles (Bartoletti *et al*., 2010; Thoreson *et al*., 2004). This allows for ribbons to provide a continual supply of vesicles for tonic release (Thoreson, 2007).

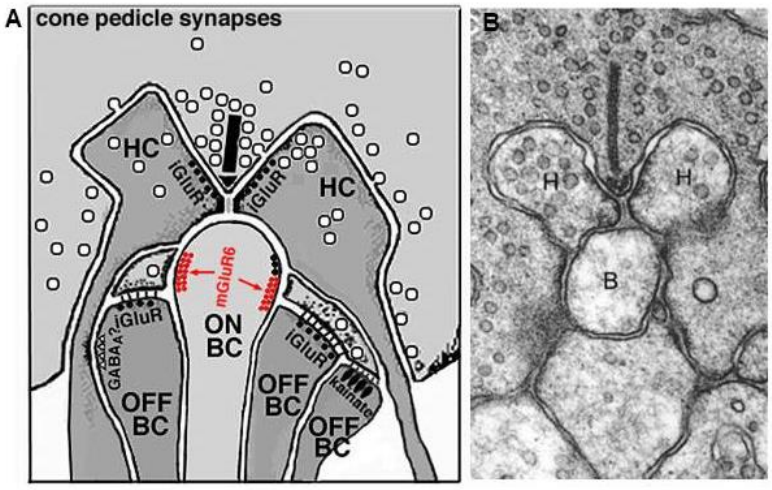

Figure 4. Cross-sectional view of cone synaptic terminal. A) Stylized image of the invaginating tripartite synapse. In mammals, the ON bipolar cell (BC) dendrite enters the center of the invagination. Two horizontal cell (HC) dendrites flank the ON BC. OFF BC dendrites terminate at flat basal contacts just outside the invaginating synapse. The locations of ionotropic glutamate receptors (iGluR) on HCs and OFF BCs and metabotropic glutamate receptors (mGluR) on ON BCs are also shown. The synaptic ribbon is represented as a black-vertical bar with white circles representing synaptic vesicles. **B)** An electron micrograph of tripartite synapse with labeled horizontal cell dendrites (H) and bipolar cell terminal **(B)**. **A)** was taken with permission, under a Creative Commons license from: "Simple anatomy of the retina" by Helga Kolb, www.webvision.med.utah.edu.Image **B)** taken from E.A. Schwartz. Transport-Mediated Synapses in the Retina. *Physiological Reviews*. 2002 Jan; 82(4):875-891.

Cone PRs release the neurotransmitter glutamate by the fusion of synaptic vesicles at ribbons (Snellman *et al*., 2010). Rods release vesicles at ribbons but can also release vesicles at non-ribbon sites (Chen *et al*., 2013, 2014). Synaptic vesicle

release from rods and cones is regulated by the gating of voltage-gated Ca^{2+} channels that are clustered just beneath the ribbon (Nachman-Clewner *et al*., 1999; Morgans, 2001; tom Dieck *et al*., 2005). Unlike conventional synapses in many neurons where release is typically regulated by activity of N- and P-type channels, release from ribbon-bearing cells (including photoreceptors) is controlled by L-type Ca^{2+} channels (Wilkinson & Barnes, 1996; Corey *et al*., 1984). L-type channels are composed of at least three subunits: an α1 pore-forming subunit together with accessory α2δ and β subunits. There is ongoing debate about whether or not γ-subunits are expressed in neurons or only in muscle cells (Chen *et al*., 2007; Dolphin, 2012). The accessory subunits affect gating properties of the channel and are involved in transport of the channel to the membrane surface (Dolphin, 2012). L-type Ca^{2+} channels are considered to be high-voltage activated channels, meaning they have a greater conductance at more positive potentials (e.g., -40 mV) as opposed to low-voltage activated channels which can open at more negative potentials (e.g., -60 mV). L-type Ca^{2+} channels are also characterized by their sensitivity to dihydropyridine antagonists and agonists. There are four types of L-type Ca^{2+} channels, Cav1.1 – 1.4 classified by the isoform of the α1 pore-forming subunit. Rod and cone PRs mainly express Cav1.4 channels (Bauman *et al*., 2004; Bech-Hansen *et al*., 1998; Strom *et al*., 1998) together with α2δ4 and β2a accessory subunits (Wysick *et al*., 2006; Ball *et al*., 2002).

L-type Ca^{2+} channels show little or no inactivation. Non-L-type Ca^{2+} channels undergo voltage-independent inactivation which allows them to close and get ready to respond to another action potential, as opposed to still transmitting the previous signal. By contrast, the persistent quality of L-type Ca^{2+} channels allows them to respond continually to graded changes in the local membrane potential. CaV1.4 channels show even less voltage- and calcium-dependent inactivation than other L-type channels (Lee

et al., 2015; Koschak *et al*., 2003; Baumann *et al*., 2004; Doering *et al*., 2005). The lack of calcium-dependent inactivation is due to the presence of an autoinhibitory domain on the C terminus (Wahl-Schott *et al*., 2006).

Glutamate release from photoreceptors causes HCs and Off BP cells to depolarize and On BP cells to hyperpolarize (Bloomfield & Dowling, 1985; Shiells *et al*., 1981). Light-evoked hyperpolarization diminishes the release of glutamate from photoreceptors, thus causes HCs and Off BP cells to hyperpolarize to light and On BP cells to depolarize to light. These different response polarities arise from differences in the glutamate receptors in these cell types. HCs and OFF BP cells contain ionotropic kainate and alpha-amino-3-hydroxy-5-methyl-4-isoxazoleproprionic acid (AMPA) receptors whereas On BP cells possess a metabotropic glutamate receptor, mGluR6 (Thoreson & Witkovsky, 1999; Yang, 2004; Snellman *et al*., 2008; Shen *et al*., 2012). Unlike ionotropic receptors in which glutamate binding opens cation channels, activation of mGluR6 by glutamate closes non-selective cation channels causing membrane hyperpolarization. By relieving this tonic hyperpolarizing influence, the cessation of glutamate release by photoreceptors in light causes On BP cells to depolarize. The transduction mechanism for mGluR6 involves release of $G_{\beta\gamma}$ subunits from G_o proteins leading to the closure of TRPM1 channels (Dhingra *et al*., 2000; Koike *et al*., 2009; Shen *et al*., 2009, 2012; Morgans *et al*., 2009). The presence of different types of glutamate receptors in different bipolar cells is important for the creation of different channels that carry different aspects of the visual scene. In addition to the different response polarities of On and Off BP cells, different Off BP cells express different populations of ionotropic glutamate receptors. Some Off BP cells express kainate receptors, some express AMPA receptors, and some express both types, albeit segregating them to different dendrites (Puller *et al*., 2013; Lindstrom *et al*., 2014; Puthussery *et al*. 2014; Borghuis *et al*., 2014). Differences in the kinetics of these different types of ionotropic glutamate

receptors contribute to differences in the abilities of BP cells to encode transient or sustained responses (Puthussery *et al*., 2014; Borghuis *et al*., 2014).

1.4 Horizontal Cell Anatomy & Physiology

HCs are interneurons that form a mosaic tiling the ONL and contacting photoreceptors throughout the OPL. HCs receive excitatory glutamatergic input from PRs and can release GABA (reviewed by Thoreson & Mangel, 2013). However, as addressed in detail later, GABA release from HCs onto photoreceptors does not appear to mediate negative feedback from HCs to cones. HCs predominately express AMPA receptors and depolarize in response to application of exogenous glutamate (Haverkamp *et al*., 2001b; Perlman *et al*., 1989). HCs in the tiger salamander seem to have only AMPA receptors (Yang I., 1998) but there is also physiological evidence for kainate receptors in HCs of human and mouse (Shen *et al*., 2004; Feigenspan & Babai, 2015). HCs are continuously activated by glutamate release in darkness allowing them to maintain a steady depolarized V_m in scotopic conditions. To do so, their iGluRs have been shown display less desensitization than iGluRs at other synapses (Perlman *et al*., 1989; Otis *et al*., 1996; Carbone & Plested, 2012). Perlman *et al*., (1989) recorded the HC V_m while applying L-glutamate for a period of 20 minutes. The HCs remained in a steady depolarized state, only hyperpolarizing during application of glutamate-free ringer (Perlman *et al*., 1989).

While cone PRs have a dark resting membrane potential between -35 to -40 mV, HCs may be depolarized to a resting potential of -10 to -30 mV in darkness and hyperpolarize by 20-50 mV in light (Dowling, 2012). Aside from HCs in fish retina, HCs do not generate sodium-dependent action potentials. The receptive field size of an individual HC is typically much larger than its dendritic field. For example, HC dendritic

fields in fish retina range from 30 to 150 μm, while their receptive fields can extend 1 to 3 mm (Stell & Lightfoot, 1975; Naka & Rushton, 1967). This difference is due to extensive electrical coupling via gap junctions between HC dendrites (Kaneko, 1971). The efficacy of the electrical coupling varies between night and day and is under neuromodulatory control that involves the release of dopamine from amacrine cells which receive their signals from ipRGCs (Lasater & Dowling, 1985; Ribelayga *et al*., 2002; Zhang *et al*., 2008).

In the primate retina, there are two types of HCs classified as H1 and H2. The cell bodies of H1 HCs receive inputs from long- and medium-wavelength cones (Verweij *et al*., 1999; Pan & Massey, 2007; Trümpler *et al*., 2008). In non-primate mammals, H1 HCs are classified as B-Type (Rodieck, 1998). The axon terminal of H1 and B-type HCs forms a compartment that is contacted only by rods and, for most part, electrically isolated from the soma and (Nelson *et al*., 1975). While largely isolated from one another, some cone signals may pass from the soma to axon compartments in B-type HCs (Trümpler *et al*., 2008). Rod inputs can pass into HC somas by traveling through gap junctions between rods and cones (Raviola & Gilula, 1973). H2 HCs are axonless cells that make contacts with S-, M-, and L- cones and are termed A-type in nonprimate species. The different subtypes of HCs form gap junctions exclusively with members of their own class as demonstrated by injection with neurobiotin (Dacey *et al*., 1996).

In lower invertebrates, HCs can be classified as luminosity (L-type) cells or chromaticity (C-type) cells (Twig *et al*., 2003). L-type HCs respond to all wavelengths of light with membrane hyperpolarization whereas C-type cells depolarize to some wavelengths and hyperpolarize to others. Mammals lack C-type HCs (Deeb *et al*., 2000). C-type HCs form a third morphological class (H3 cells; Negishi *et al*. 1997). Although there appears to be only a single morphological class, there are two physiological types

of C-type HCs: biphasic R/G cells (which hyperpolarize to green light but depolarize to red light) and triphasic cells (which hyperpolarize to red and blue but depolarize to intermediate green wavelengths) (Burkhardt, 1993).

Salamanders contain A- and B-types of HCs, in parallel to subtypes found in mammals. In salamander, A-types (H2) received signals exclusively from cones, while both the soma and axon terminal compartments of B-types (H1) received mixed rod/cone signals (Zhang *et al*., 2006). We did not distinguish these subtypes in our experiments. We found that as long as there was evidence of feedforward connections from cones to HCs, we observed negative feedback effects from HCs to cones, suggesting that all subtypes participate in HC feedback.

1.5 Lateral inhibitory feedback from HCs to photoreceptors

Hartline was awarded the Nobel Prize in 1967 for the discovery of lateral inhibition in the retina of the horseshoe crab, *Limulus polyphemus* (Hartline *et al*., 1956; Ratliff & Hartline, 1959). Hartline *et al*. examined the responses of individual photoreceptors while stimulating neighboring neurons with light. They noticed an exponential increase in action potential frequency (as opposed to a linear increase) from the recorded neuron as the light approached closer and closer to a neighboring photoreceptor. When the light finally reached an immediately adjacent cell, the recorded PR became strongly inhibited and greatly reduced its firing rate (Hartline *et al*., 1956; Dowling, 2012). Lateral-inhibitory feedback was subsequently shown to be important in other sensory systems besides vision. In somatosensation, lateral inhibitory feedback improves two-point discrimination or the ability to distinguish to between two spatially different points of tactile sensation (von Békésy, 1967). Lateral inhibition helps to refine and narrow the signals, thus decreasing overlap and increasing the spatial resolution,

much like decreasing the optical point spread function in microscopy (Kandel *et al*., 2000).

Denis Baylor *et al*. (1971) showed that HCs mediate lateral inhibition to cone PRs in vertebrate retinas (Fig. 5). While hyperpolarizing cone PRs with a spot of light under current clamp conditions, Baylor *et al*. noticed that increasing the diameter of a light stimulus caused the cone's membrane potential to depolarize. The kinetics and receptive field properties of these depolarizing responses in cones were similar to those of HC light responses. To test for a connection between the two cell types, they polarized the membrane of a HC while recording the membrane potential in a nearby photoreceptor. They observed a sign-inverting signal between cones and HCs and concluded that the depolarizing response in cones was due to HC hyperpolarization (Baylor *et al*., 1971).

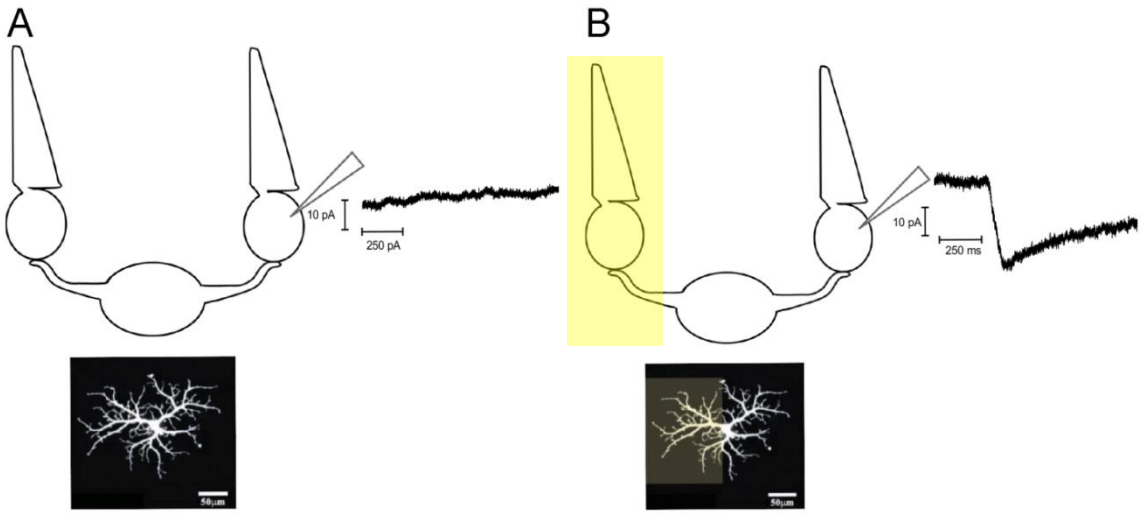

Figure 5. Lateral-inhibitory feedback from a HC to a cone PR. The effect on the cone I_{Ca}. **A)** A diagram of two cone PRs with a HC. The cone on the right is voltage clamped and the trace represents a recording of the membrane while the cone is in dark. Below, is an A-type HC filled with neurobiotin from the rabbit retina. **B)** Same schematic, only the left-hand side of the HC (below) is illuminated. This causes the HC to hyperpolarize which relieves inhibitory feedback to the cone, causing an increase in I_{Ca} and development of an inward current (represented by a downward deflection of the trace on the right). Traces recorded by Ted Warren and Wallace B. Thoreson. A-type HC taken with permission from Pan F, SL Mills, SC Massey. Screening of gap junction antagonists on dye coupling in the rabbit retina. Visual Neuroscience. 2007 Jul-Aug;24(4):609-18, reproduced with permission.

Feedback from HCs to PRs is critical for comparing local and global changes in light intensity. With their wide receptive field, HCs collect information from many cones and thus measure the average luminance over a wide area of the retina. By feeding an inhibitory signal back onto a PR terminal, the response to the average light level is subtracted from the response of that individual photoreceptor so that intensity changes which exceed background become more salient. For example, imagine a white bar falling on only one small region of the HC receptive field. Because cones are hyperpolarized by light, the HC will be receiving less glutamate from the illuminated cones compared to nearby cones in darkness. The HC feeds back an adjusted inhibitory signal onto cone PRs in the dark region, disinhibiting I_{Ca} and thereby increasing glutamate release. This enhances the dark border to make it appear extra-dark. This mechanism underlies the perceptual phenomenon known as Mach bands, where the perceptual contrast between a light and dark border is enhanced (Thoreson & Mangel, 2012).

Subtraction of surrounding average light levels from local changes by lateral-inhibitory feedback creates antagonistic center-surround receptive fields. These circular receptive fields were first discovered in cat RGCs by Stephen Kuffler (1953) who showed that shining a spot of light the size of the dendritic field on certain RGCs

increased their firing rate, while shining an annulus that extended further into the periphery inhibited responses. Center-surround receptive fields appear first in cones and are also found in BP cells and lateral geniculate neurons that are downstream from RGCs (Wiesel & Hubel, 1966). The appearance of center-surround receptive fields in cones and the ability of compounds that block HC feedback to abolish this organization in RGCs suggests that center-surround receptive fields originate with negative feedback from HCs to cones (Mangel, 1991; Witkovsky *et al*., 2006; McMahon *et al*., 2004).

Lateral inhibitory feedback not only helps us to detect edges and borders but also contributes to local adaptation. In everyday visual scenes there is a great range of luminance between different objects within the visual scene and if PRs were to directly read out the light signals falling on them with no comparison, some individual objects could become saturated and it would impossible to distinguish bright objects from dimmer ones (Rodieck, 1998). This is akin to what happens when one photographs a bright object in a dim room (Masland, 2013). HC feedback provides local control of amplification of spatially disparate signals, allowing the retina to view all objects, even if one is emanating or reflecting far more photons than another object in the same visual scene.

Feedback from HCs to cones is also critical for detecting color by creating what are known as color opponent center-surround fields. Color vision requires the comparison of signals from different cones with differing spectral sensitivities. Although cones can differ in their spectral sensitivity, individual cones are “color blind” (Baylor *et al*., 1987). This means that individual cones, regardless of their spectral sensitivity, respond to the number of photons caught by their photopigments. The spectral sensitivity of the photopigment in a cone increases the probability that certain wavelengths will be absorbed over others, but if one increases the intensity of a light,

this has the effect of increasing the probability that the photon will be caught by the PR. The idea that cone responses vary only with the number of photons that is captured and not with the wavelength of those photons is referred to as the principle of univariance (Rushton, 1972). It is only by comparing the ratios of photons caught by cones with differing spectral sensitivities that color differences can be detected. Lateral inhibitory interactions between individual cones and HCs allow for this comparison and create color opponent responses. Recall that C-type HCs respond with different polarities to different wavelengths of light. L-type HCs, on the other hand, respond to all wavelengths of light with hyperpolarization. Thus, the hyperpolarization of red-sensitive cones to red light causes post-synaptic L-type HCs to hyperpolarize. Both red and green-sensitive cones receive inhibitory feedback from L-type HCs. Hyperpolarization of L-type HCs by red light thus relieves inhibitory feedback from L-type HCs onto green-sensitive cones. The increased glutamate release from green-sensitive cones produces a depolarizing response to red light in color-opponent HCs receiving synaptic inputs from these cones. In support of a role of HC feedback in generating color opponency in the retina, blocking HC feedback eliminates color opponent responses in HCs as well as RGCs (Vigh & Witkovsky, 1999; Crook *et al*., 2011; Kamiji *et al*., 2012).

In addition to feedback onto cone terminals, HCs also supply inhibitory feedback to rod PRs (Babai & Thoreson, 2009; Thoreson *et al*., 2008). The mechanisms of HC feedback to rods appear similar to feedback from HCs to cones (Thoreson *et al*., 2008). Although it has not yet been investigated, the role(s) of HC to rod feedback in retinal processing are also likely to be similar. For example, HC to rod feedback may contribute to formation of center-surround receptive fields in retinal ganglion cells under scotopic or mesopic conditions (Thoreson & Mangel, 2012).

HCs can also supply positive feedback back to cone terminals (Jackman *et al*.,

2011). This positive feedback is not well understood but involves activation of AMPA receptors in HCs and is thought to involve more spatially-limited local interactions than negative feedback. By countering the global suppression of cone glutamate release by negative feedback in locally juxtaposed cones, this positive feedback mechanism may improve our ability to detect faint details at a border or an edge (Jackman *et al*., 2011).

1.6 Mechanisms of negative feedback from HCs to cones.

As stated earlier, cone terminals contain L-type Ca^{2+} channels that open upon membrane depolarization and allow Ca^{2+} to come into the terminal and ultimately cause fusion of glutamate-laden synaptic vesicles with the membrane. It was recognized quite early that the depolarizing influence of HC to cone feedback modulated the I_{Ca} at the cone terminal (Gerschenfeld & Piccolino, 1978; Piccolino & Gerschenfeld, 1978; Byzov, 1979; Gershenfeld *et al*., 1980), but it was not until 1996 that Verweij *et al*. determined exactly what aspects of the cone I_{Ca} was being modulated. Verweij *et al*. used voltage-clamp intracellular recordings from cones to step the cone V_m to various potentials and compiled two current vs. voltage relationships (hereafter, referred to as an I-V plot), one where a small spot of light illuminated only the recorded cone and one where an annulus was also present to illuminate the surrounding retina. Application of annular illumination did not produce further changes in the cone since it was already saturated by bright central illumination but instead hyperpolarized surrounding HCs that have very large receptive fields. Upon hyperpolarization of HCs by annular illumination, inhibitory feedback was diminished and the activation curve of the cone I_{Ca} shifted leftward on the I-V plot to more negative potentials (Fig. 6). This was subsequently confirmed by others (Hirasawa & Kaneko, 2003; Cadetti & Thoreson, 2006).

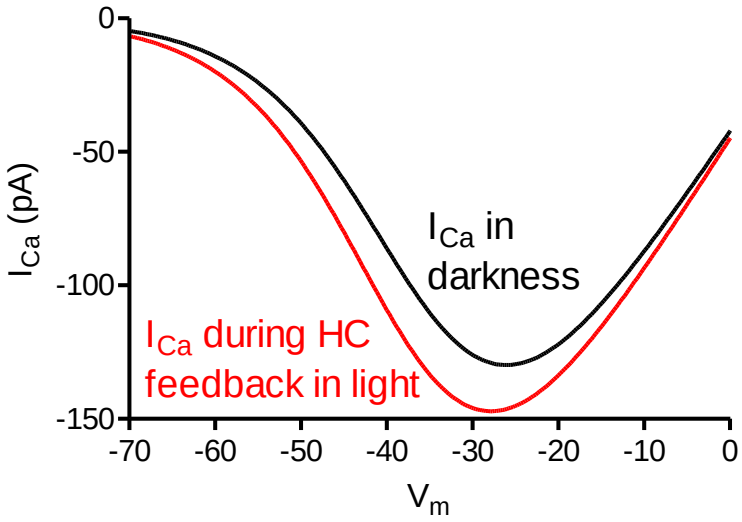

Figure 6. Cone I_{Ca} with and without feedback. A representative I-V plot of cone I_{Ca} in darkness (black trace) and during surround illumination (red-orange trace). Notice the increase in the peak current and the shift in the activation voltage for I_{Ca} to more negative membrane potentials during surround illumination.

Since visual information is encoded in the amount of release of the neurotransmitter glutamate from the cone terminal, a change in activity of L-type Ca^{2+} channels will alter the amount of glutamate release (Fig. 7). Light-adapted cones have a membrane potential of around -45 to -50 mV, just below the mid-point of the I_{Ca} I-V plot. Thus, a small leftward shift in activation induced by the reduction of HC feedback in light can cause a significant increase in I_{Ca} activation even without any change in the cone membrane potential. Conversely, depolarization of HCs in darkness will cause a positive (rightward) shift in activation, thereby decreasing I_{Ca} and glutamate release from cones.

Although it was discovered more than 40 years ago, there is still no consensus concerning the mechanism by which HCs mediate inhibitory feedback onto PRs (Fig. 7). The three main theories are: 1) a synaptic mechanism (i.e., HC release of GABA onto PR terminals), 2) a pH modulatory mechanism (i.e., a change in the synaptic cleft pH), and 3) an ephaptic mechanism (i.e., HC polarization influences the local electric field

surrounding the voltage-sensitive L-type Ca^{2+} channels).

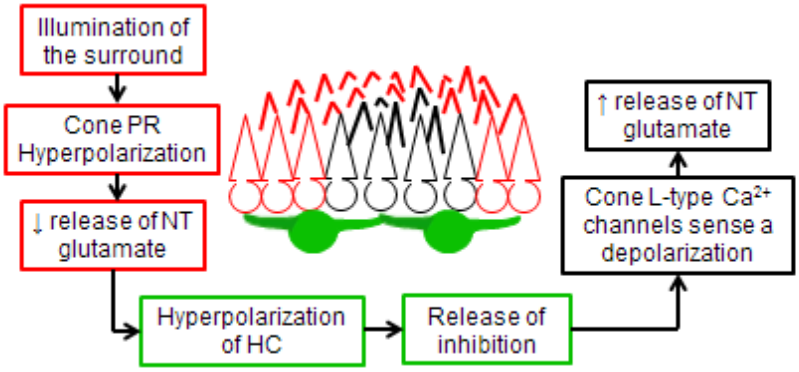

Figure 7. Flowchart of lateral-inhibitory feedback in the outer retina. The red-colored cones represent an illuminated surround. The green neurons are the HCs, which in this case become hyperpolarized upon illumination of the surround. This hyperpolarization leads to a disinhibitory effect on L-type Ca^{2+} channels within the synaptic terminals of the cone PRs in the center (black) which in turn increases their release of glutamate. This mechanism creates center-surround antagonistic receptive fields that can also be observed in downstream BP and RGCs.

uptake of GABA compared to other retinal cells and dark-adapted HCs (Lam & Steinman, 1971; however, see Lam, 1975 for exceptions to this). Both vertebrate and invertebrate HCs contain GABA, GABA-synthesizing enzyme glutamic acid decarboxylase (GAD), and GABA transaminase (see Thoreson & Mangel, 2012). HCs also contain SNARE and other proteins (e.g., SNAP25, syntaxin-4) involved in synaptic release within their dendritic arbors (Lee & Brecha, 2010; Hirano 2007, 2011). Upon stimulation with glutamate and its agonists, HCs have been shown to release GABA. There is curious evidence that release of GABA can occur via Ca^{2+}-independent mechanism (Yazulla & Kleinschmidt, 1983; Schwartz, 1982). This Ca^{2+}-independent mechanism relies on the GABA transporter being present within HC dendrites (Schwartz, 2002). A possible mechanism by which this could occur comes from the neuromuscular junction where there is non-vesicular release of acetylcholine that is mediated by vesicular acetylcholine transporters following vesicle fusion with the plasma

membrane (Petrov *et al*. 2011). Similarly, the vesicular GABA transporter may be situated within the vesicle membrane to direct GABA into the vesicular lumen. Upon exocytosis, the side of the transporter that was facing the lumen is now exposed to the synaptic cleft and able to transport GABA into the cleft without Ca^{2+} being involved. However, this non-canonical form of neurotransmitter release seems to be limited to non-mammalian species since these GABA transporters were not found in guinea pig HCs (Guo *et al*., 2010).

Tachibana and Kaneko (1984) reported that isolated red- & green-sensitive cones from fresh-water turtles showed an increase in Cl^- currents upon application of GABA. In blue-sensitive cones and rod PRs, no effects were seen (Tachibana & Kaneko, 1984). Together with evidence that HCs can release GABA, this suggested that perhaps GABA receptors might mediate HC to cone feedback. Wu (1991) found in salamander cones that had lost their OS that an application of the GABAa antagonist, bicuculline, blocked HC to cone inhibition. However, studies from a variety of other species found that HC feedback onto cones was unperturbed by application of GABA, GABA antagonists, or GABA agonists (Thoreson & Burkhardt, 1990, Verweij et al., 1996, Hirasawa & Kaneko, 2003; Verweij et al., 2003, Tatsukawa *et al*., 2005; Crook *et al*., 2009, 2011). Center-surround receptive fields of BP cells and RGCs in primate and salamander retina were also unaffected by a variety of GABA antagonists (Hare & Owen, 1996; McMahon *et al*., 2004).

Other evidence against the GABA hypothesis concerns the reversal potential of Cl^- (E_{Cl}) in cone PRs. In the dark, cone E_{Cl} is approximately -37 mV (Thoreson & Bryson, 2004). The driving force on a particular ion is the difference between the resting membrane potential and the ion's reversal potential ($V_m - E_{rev}$). So, at potentials more negative than E_{rev} (-37 mV), Cl^- will flow out of the cone and cause a membrane

depolarization. In bright light, cone PRs have a resting V_m ≈ -45 mV and so release of GABA from HCs Cl^- should depolarize cones, not hyperpolarize them as predicted for inhibitory feedback from HCs to cones. Thus, a large body of evidence argues that GABA is not a viable candidate for lateral-inhibitory feedback from HCs to cones (Dowling, 2012).

2. The Ephaptic Hypothesis

The idea that an ephaptic or purely electrical mechanism can influence cell-to-cell communication has its roots as far back as the 1930's. At the time, neurophysiologists were debating whether neurons communicated to one another via chemical or electrical means (the so-called "soup v. spark" debate; Faber & Korn, 1989). While chemical communication is the principal means by which neurons communicate with one another, purely electrical communication through gap junctions is also quite important (Pereda, 2014). Ephaptic communication appears to be more limited and has thus received less attention (Anastassiou and Koch, 2015). The term ephaptic comes from the Greek word ἑφάψή, meaning "touch or junction" (Arvanitaki, 1942). Ephaptic processes are classified into two different categories, 1) those generated from the synchronous activity of a network or an ensemble of neurons, and 2) those between two different neuronal cell types (Faber & Korn, 1989). The former, which are largely excitatory are seen at the neuronal network level, while the latter is usually inhibitory and at the individual level of the neurons themselves (Jefferys, 1995; Anastassiou & Koch, 2015). To date, there are only a few confirmed examples of ephaptic coupling between individual neurons. They include the Mauthner cell axon cap in teleost, the pinceau of the cerebellar Purkinje cell, layer 5 pyramidal neurons of the neocortex, the photoreceptors of the blowfly, and compartmentalized olfactory receptor neurons in

Drosophila (Korn & Faber, 2005; Blot & Barbour, 2014; Anastassiou *et al*., 2011; Weckström & Laughlin, 2010; Su *et al*., 2012).

At the tripartite photoreceptor synapse, polarization of the HC had little or no effect on the cone's overall V_m, but instead altered the cone I_{Ca} (Byzov & Shura-Bura, 1986; Piccolino & Neyton, 1982). The increase in I_{Ca} at the cone terminal that is induced by HC's inhibitory feedback could not be readily explained by a conventional synaptic mechanism and so it was instead postulated that it might be due to either an ephaptic or neuromodulatory mechanism (Byzov, 1979; Gerschenfeld *et al*., 1980; Piccolino & Neyton, 1982).

In the ephaptic mechanism envisioned by Byzov, upon HC hyperpolarization, current flow into the HC through the extracellular resistance in the synaptic cleft generates a local voltage drop or a net negative field within the synaptic cleft. This reduction in positive charge within the synaptic cleft would effectively depolarize the locally adjacent cone membrane. This highly local depolarization of voltage-gated Ca^{2+} channels (VGCC) would explain the decrease in threshold for activation of cone I_{Ca} upon HC hyperpolarization. The ephaptic hypothesis is supported by the fact that the cleft size of the tripartite synapse is narrower than traditional synapses (~16-20 nm compared to ~30 nm; Dowling, 2012), which could produce a higher cleft resistance and thus a larger voltage drop between the interior of the invaginating synapse and the surrounding extracellular space. However, some critical parameters have not been measured and so this is only circumstantial evidence for an ephaptic mechanism (Dowling, 2012). The resistance of the HC dendrite and its space constant (λ) are key parameters in determining if an ephaptic event is feasible at this synapse but they remain unknown (Dmitriev & Mangel, 2006; Anastassiou & Koch, 2015). Resistance of the extracellular matrix is also unknown. This resistance is determined by both its chemical composition

and the cleft volume. Because of a lack of detailed ultrastructural data at the cone synapse, current models of the ephaptic effect do not take into account cleft volume sizes (Gardner *et al*., 2015). Although the cleft is narrow, the dendrite of the HC within the rod PR terminal has an alternating “ballooned” and “crinkled” topology yielding a rather large total surface area of 5.1 ± 1.2 μm^2 (Rao-Mirotznik *et al*., 1995). The cleft volume within the rod invagination is thus 20-fold greater than an average synaptic bouton (Rao-Mirotznik *et al*., 1995). A similarly large volume is present at cone invaginations and this large volume would reduce the overall extracellular resistance, reducing the ability of extracellular current flow to produce ephaptic voltage changes.

Kamermans *et al*. (2001) proposed a modification to the ephaptic mechanism in which the HC current sink involved hemi gap junctions or hemichannels at the tips of the HC dendrites. Gap junctions are formed from two hemichannels or connexons. Each connexon is composed of six transmembrane subunits known as connexins which are arranged in such a way as to form a pore in the membrane. While many hemichannels remain closed in the absence of a partner, some hemichannels are capable of opening into the extracellular space to allow current to pass across the cell membrane (Sáez *et al*., 2005). Immunohistochemical evidence for hemichannels at the dendritic tips of HCs along with a lack of ultrastructural evidence that these hemichannels formed gap junctions with other hemichannels prompted the idea that they might be involved in ephaptic feedback (Janssen-Bienhold *et al*. 2001; Kamermans *et al*., 2001).

In support of a role for hemi gap junctions in feedback, a connexon antagonist carbenoxolone reduced feedback (Kamermans *et al*., 2001). However, carbenoxolone also has effects on many other mechanisms including direct inhibition of L-type Ca^{2+} channels in cones (Vessey *et al*., 2004). Thus, carbenoxolone inhibits transmission from cones to HCs making it difficult to separate effects on HC feedback to cones from effects

on cones to HCs when using light stimuli. To examine feedback directly without the use of light responses, Cadetti and Thoreson (2008) simultaneously voltage-clamped both a cone and HC. Polarizing the HC caused changes in the voltage-dependence and amplitude of I_{Ca} similar to those produced by polarizing HCs with annular illumination. However, blocking hemi gap junctions with carbenoxolone did not reduce the feedback effects of HC polarization on cone I_{Ca} (Cadetti & Thoreson, 2008).

In another approach, Shelley *et al*. (2006) knocked out the HC gap junction protein, connexin 57, in mice. This caused a reduction in contrast sensitivity but this reduction was attributed to blocking the coupling between HCs and thus reducing the size of their receptive fields (Shelly *et al*. 2006). Feedback is reduced when the size of the illuminating surround is reduced (Kaneko & Hirasawa, 2003).

Eliminating the major gap junction protein in zebrafish HCs, connexin 55.5 also reduced contrast sensitivity (Klaassen *et al*., 2011). In addition, consistent with a role in negative feedback from HCs, loss of this protein eliminated depolarizing responses in color-opponent HCs and reduced changes in cone I_{Ca} voltage-dependence induced by HC depolarization (Klaassen *et al*., 2011). Thus, it has been suggested that in zebrafish, HC feedback may involve ephaptic mechanisms utilizing connexin 55.5.

As illustrated in Fig. 6, inhibitory feedback from HCs causes both a change in the threshold of activation and a change in the peak amplitude of cone I_{Ca} (Verweij *et al*., 1996; Kaneko & Hirasawa, 2003; Cadetti & Thoreson, 2006; Thoreson *et al*., 2008; Packer *et al*., 2010). A purely ephaptic mechanism will not produce a change in the peak amplitude of I_{Ca}. Kaneko and Hirasawa (2003) showed that adding an additional depolarization (+2 mV) to the cone to simulate an ephaptic effect caused appropriate shifts in the voltage activation threshold but did not produce the increase in the peak of I_{Ca} that is consistently seen with HC hyperpolarization. Thus, while there may be an

ephaptic contribution to HC feedback, there is also a significant contribution from other mechanism(s) (Wang *et al*., 2013; Vroman *et al*., 2014).

Ephaptic changes can occur at the speed of light and are thus effectively instantaneous. An ephaptic mechanism may be measured relative to a slower event (e.g., synaptic transmission) or by observing if the measured phenomenon is as fast as the time-resolution capabilities of the electrode (Blot & Barbour, 2014; Ogden, 1987). Light responses of HCs and light-evoked feedback changes in cones showed nearly identical kinetics, leading to the suggestion that a component of HC feedback is instantaneous (Vroman *et al*., 2013, 2014). However, HC light responses are intrinsically slow and thus limit the resolution of these comparisons. To test for contributions from an ephaptic mechanism, we examine the kinetics of HC feedback in Chapter 2 using voltage clamp techniques to rapidly change the HC membrane potential while simultaneously measuring feedback-induced changes in I_{Ca} in cones.

3. The pH Hypothesis

Protons are a potential candidate for the fast-acting, neuromodulatory substance that Gershenfeld *et al*. (1980) suggested was involved in HC feedback. Protons have inhibitory effects on the conductance of Na^+ and Ca^{2+} channels (Ohmori & Yoshii, 1977; Prod'hom *et al*., 1987; Hess *et al*., 1986; Tang *et al*., 2014). Individual protons are capable of blocking the channel pore or exerting electrical effects on the voltage-sensing helix of the channel, thus affecting its conductance (Prod'hom *et al*., 1987; Chen & Tsien, 1997). In studies on salamander cones, Barnes *et al*. (1993) showed that increasing the extracellular pH from 7.0 – 8.2 caused an increase in the peak amplitude of L-type I_{Ca} and lowered the threshold for activation. They concluded that a change in the proton concentration of the cleft has a modulatory effect on the gain of synaptic

transmission, consistent with a potential role of these ions in feedback.

An increase in the number of protons in the cleft can alter the membrane surface potential. Head groups of phospholipids that make up the lipid bilayer have a net negative charge that can be neutralized by the binding of a positively charged ion (e.g., divalent cation or proton). Thus, if one decreases the concentration of Ca^{2+} or protons to remove that counter ion from the membrane, this makes the external surface of the membrane more negative, diminishing the voltage drop that occurs between the outer and inner membrane surfaces. This effectively depolarizes the membrane without adding more positive charges to the inner membrane (Hille, 2001). Surface charge theory can account for the voltage shifts in I_{Ca} activation induced by protons (Krafte & Kass, 1988; Zhou & Jones, 1996). However, the fact that different Ca^{2+} channel subtypes respond to pH changes with different magnitude voltage shifts suggests that these shifts are not entirely due to diffuse surface charge effects (Doering & McRory, 2007). A local increase in protons near the voltage sensor could offset negative charges around the voltage sensor and thus increase the local trans-membrane electrical field experienced by the VGCC to produce a rightward shift in the threshold for activation of I_{Ca}.

To account for pH effects on the amplitude of I_{Ca}, Chen and Tsien (1997) provided evidence that protons can transiently block the pore by competitively binding with negatively charged glutamate residues within the pore. These residues are responsible for the initial binding and selectivity for Ca^{2+} ions to be transferred across the pore. Modified VGCCs where aspartate residues were substituted for glutamate residues in the pore showed less of a pH effect on channel conductance than wild type channels (Chen & Tsien, 1997). The idea is that protons interfere with the binding of Ca^{2+} ions to the selectivity filter of the channel and this is measured as a decrease in I_{Ca} (Tang *et al*.,

2014).

To test a role for pH in feedback, Kaneko and Hirasawa (2003) supplemented the bicarbonate buffer of the external medium with the pH buffer, 4-(2-hydroxyethyl)-1-piperazineethanesulfonic acid (HEPES; pK_a = 7.5). Upon stimulation with a light annulus to activate the surround, limiting pH changes in the cleft with 10 mM HEPES eliminated the effects of HC feedback on the cone I_{Ca} (Kaneko & Hirasawa, 2003). HC feedback assessed with paired cone/HC recordings and by Ca^{2+} imaging techniques was also abolished by supplementing the superfusate with HEPES (Cadetti & Thoreson, 2006; Vessey *et al*., 2005). HC feedback to rods was also eliminated by HEPES (Thoreson *et al*., 2008; Babai & Thoreson, 2009). Packer *et al*. (2010) showed that the center-surround antagonistic receptive fields of On retinal ganglion cells were abolished by supplementing bicarbonate with HEPES. Color-opponency in the retina of primates and fish is also blocked by HEPES (Crook *et al*., 2011; Kamiji *et al*., 2012).

In dissociated HCs, Fahrenfort *et al*. (2009) found that application of HEPES caused an intracellular acidification and suggested that this intracellular acidification might have adverse effects on connexin channels. However, Kaneko and Hirasawa (2003) showed that the non-aminosulfonate buffer 2-Amino-2-hydroxymethyl-propane-1,3-diol (Tris) also eliminated feedback. In addition, Trenholm and Baldridge (2010) demonstrated that buffers that possess aminosulfonate groups but exhibit buffering capabilities outside of the extracellular pH range had no effect on HC feedback. Furthermore, those buffers that did not buffer within the normal pH range nevertheless caused intracellular acidification. These data indicate that the block of feedback was not due to direct or indirect pH-mediated effects of aminosulfonate buffers on connexins.

Jouhou *et al*. (2007) used a pH-sensitive dye, 5-hexadecanoylaminofluorescein (HAF), to measure near-membrane pH changes in dissociated HCs from fish retina.

They found that depolarization of HCs caused extracellular acidification. However, a later study by Jacoby *et al*. (2014) showed under the conditions used by Jouhou *et al*., his dye likely reported near-membrane intracellular pH, not extracellular pH. When loaded for shorter periods of time, Jacoby *et al*. (2014) found that HAF reported extracellular alkalinization upon HC depolarization. This was consistent with earlier observations by the same group made with pH-sensitive electrodes in which they found that depolarization of dissociated HCs caused extracellular alkalinization (Jacoby *et al*., 2010). These findings are opposite to predictions for a role of protons in mediating HC feedback to cones. However, the cell dissociation process may have sheared off critical cellular elements at the tips of the HC dendrites. To measure pH changes in a more intact retina preparation, Wang *et al*. (2013) measured changes in synaptic cleft pH by engineering a double transgenic zebrafish carrying a pH-sensitive molecule, calipHluorin, attached to the α2δ4 subunit of the L-type Ca^{2+} channel which is anchored on the extracellular face of the cone membrane. Wang *et al*. (2014) also generated HCs to express invertebrate FMRF-amide receptor Na^{+} (FaNaC) channels. Upon imaging flatmount retinal tissue, they observed alkalinization of the synaptic cleft when HCs were hyperpolarized by light and acidification when HCs were depolarized by activation of FaNaC channels with FMRF-amide. This study provided direct evidence for changes in the synaptic cleft pH with HC polarization that are consistent with the pH hypothesis.

The experiments described above establish a critical role for protons in HC feedback to cones by showing that: 1) extracellular pH changes can reproduce the effects of feedback, 2) blocking pH changes eliminate feedback, and 3) appropriate pH changes are observed in the synaptic cleft. In the following chapter, we examine three questions concerning HC feedback to cones. 1) What is the source of extracellular protons that are involved in HC feedback? 2) What is the mechanism by which free

protons are removed by HC hyperpolarization? 3) Are the kinetics of feedback fast enough to support involvement of an ephaptic mechanism?

Chapter 2: Results

2.1 Introduction

The retina has two principal functions: 1) to transduce a light signal into an electrochemical signal and 2) to compare signals between different neurons (Rodieck, 1998). Both of these functions are initially performed by photoreceptor cells which can catch photons of light and respond with graded changes in their membrane potential (V_m) that reflect the number of captured photons. These light-evoked changes in membrane potential in turn regulate release of the neurotransmitter glutamate and thus convey analog information of the visual scene to downstream neurons and ultimately to the brain. However, PRs do not simply convey differences in light intensity of the visual scene, but also have their signals modified by neighboring PRs through interactions with interneurons known as horizontal cells (HCs). By allowing PRs to compare signals between one another, these interactions shape contrast and chromatic sensitivity.

HCs that mediate these lateral interactions between photoreceptors receive inputs from a spatially extensive array of PRs. In addition to feedforward inputs from PRs, HCs also make inhibitory feedback connections back onto PRs that modulate the activity of L-type Ca^{2+} channels in PR terminals, thus altering the amount of glutamate release (reviewed by Thoreson & Mangel, 2012). By subtracting the spatially averaged luminance signal received from many surrounding PRs, negative feedback from HCs to individual PRs enhances the detection of local differences in light intensity, thereby improving the salience of borders and edges. Negative feedback interactions between spectrally distinct cone subtypes can also create color opponent responses (Packer *et al*., 2010; Crook *et al*., 2011).

The mechanism by which HCs supply inhibitory feedback to cone PRs has been debated since its discovery over 45 years ago (Baylor *et al*., 1971). Although other

mechanisms may also contribute, experiments from a number of different laboratories have established a role for protons. Key results include the ability of pH changes to replicate feedback effects on cone I_{Ca} (Barnes *et al*., 1993), blockade of HC feedback by enhanced pH buffering (Hirasawa & Kaneko, 2003; Vessey *et al*., 2005; Cadetti & Thoreson, 2006; Trenholm & Baldridge, 2010), and the demonstration that HC depolarization acidifies the cone synaptic cleft (Wang *et al*., 2013). A major goal of the present study was to determine the source(s) of protons involved in HC feedback to cones. There are only a few mechanisms by which extracellular protons can be generated in the synaptic cleft. The most likely possibilities are: 1) generation of protons by the actions of extracellular carbonic anhydrase (CA), 2) exocytotic release of protons that are packaged into synaptic vesicles with anionic neurotransmitters, and 3) extrusion of protons by Na^+/H^+ exchangers (NHE). The experiments described in this study point to a Na^+/H^+ exchanger (NHE) within the HC membrane as the principal source of protons for lateral-inhibitory feedback. Although NHEs provide the major source for extracellular protons, NHEs are not voltage-dependent (Fuster *et al*., 2004). Instead, our results further suggest that voltage-dependent changes in synaptic cleft pH caused by HC voltage changes involve bicarbonate flux across the HC membrane.

In addition to contributions from protons, there is also evidence for a second component to feedback (Vroman *et al*., 2014) that may involve an ephaptic mechanism (Byzov & Shura-Bura, 1986; Kamermans *et al*., 2001). The current idea is that gap junction hemichannels in HC dendrites allow greater inward current flow when HCs hyperpolarize (Vroman *et al*., 2013). When combined with high extracellular resistance, this current flow can create a voltage drop within the synaptic cleft. By making the local electrical field inside the synaptic cleft more negative, this reduces the local trans-membrane voltage drop sensed by L-type Ca^{2+} channels in the cone terminal, allowing

them to activate at more negative potentials. One property of ephaptic voltage changes is that they occur instantaneously (Jefferys, 1994; Vroman *et al*., 2013). Consistent with this prediction, Vroman *et al*. (2014) found that the kinetics of feedback currents in cones evoked by annular illumination matched the kinetics of HC light responses. However, HC light response kinetics are themselves relatively slow and thus may become the rate-limiting step in this comparison. To produce rapid changes in HC membrane potential, we measured the kinetics of feedback currents in cones evoked by voltage steps applied simultaneously to voltage-clamped HCs. Consistent with Vroman *et al*. (2014), we found two kinetic components to feedback but both components were too slow to be explained by a purely ephaptic mechanism.

2.2 Methods

Preparation

Negative feedback from HCs and cone PRs was studied using two different preparations of salamander retina: flatmount and slice preparations. In both instances, euthanasia of the animal was done in an ethical manner in accordance with the protocols approved by the University of Nebraska Medical Center and the Institutional Animal Care and Use Committee.

Adult-aquatic tiger salamanders (*Abystoma tigrinum*, 18 – 25 cm in length, male or female, Charles D. Sullivan, Co., Nashville, TN, USA) housed on a 12 hour-light/day cycle. Experiments were begun 1-2 h into subjective night. Salamanders were anesthetized by immersion in MS222 (0.25 g/L) for >15 min and then decapitated with heavy shears. The head was hemisected and the spinal column rapidly pithed. The eyes were then enucleated and nested on a saline-soaked cotton wad placed on a linoleum block for ease of dissection (Van Hook & Thoreson, 2013). The anterior portion of the

eye was removed and the eyecup was quartered. For the retinal slice preparation, the eyecup quarters were placed on a rectangular piece of nitrocellulose paper (5 x 10 mm; type AAWP, 0.8 µM pores, Millipore Ltd.) and then the retinas were isolated from the retinal pigment epithelium, choroid and sclera. The filter paper with retina was cut into strips with a width of 125 µm. The retinal slices were rotated 90 degrees and placed in the recording chamber where they were perfused at ~1 ml min-1 with a pH 7.4 bicarbonate-buffered Ringer solution (all in mM: 101 NaCl, 22 $NaHCO_3$, 2.5 KCl, 2.0 $CaCl_2$, 0.5 $MgCl_2$, 11 glucose). Solutions were continuously bubbled with 95% O_2/5% CO_2. In some experiments, $NaHCO_3$ was changed to 12 or 32 mM to achieve solution pH of 7.1 or 7.8, respectively. In these solutions, the amount of NaCl was adjusted to maintain an osmolality of 240 – 244 mOsm as assessed by an osmometer (Wescor). We prepared a nominally-Na^+ free solution by replacing Na^+ with choline (all in mM: 101 Choline-Cl, 22 Choline-HCO_3, 2.5 KCl, 2.0 $CaCl_2$, 0.5 $MgCl_2$, 11.0 glucose, bubbled for 10 min with 95% O_2/5% CO_2). For HEPES experiments, we added 10 mM HEPES to the standard bicarbonate-buffered solution without adjusting the osmolality and used NaOH to return the pH to 7.4. For bafilomycin experiments, we incubated the eyecup overnight at 4ºC in a 1% BSA-bicarbonate buffered saline solution to preserve the tissue's vitality. The chamber was viewed with a water-immersion objective (40X, 0.7 NA) on an upright-fixed stage microscope (BH-2 RFCA Olympus).

In order to record light responses from the flatmount retina preparation, we prepared the tissue in the dark with the aid of infrared illumination and dissecting microscope (Bausch and Lomb) equipped with night-vision goggles (NiteMate NAV3, Litton). A section of dark-adapted, isolated retina was placed ganglion cell layer down onto a piece of nitrocellulose membrane with a small rectangular hole in the center to allow for light stimuli to be focused on the photoreceptors.

Electrophysiology

Patch pipettes for whole-cell patch clamp recordings were pulled from borosilicate glass (1.2 mm o.d., 0.95 mm i.d., with an internal filament, World Precision Instruments, Sarasota, FL, USA) using a PP-830 micropipette puller (Narishige, Tokyo, Japan). Pipettes were filled with an internal-recording solution containing (in mM): 50 Cs-Gluconate, 40 Cs-Glutamate, 40 CsOH, 10 TEA-Cl, 3.5 NaCl, 1 $CaCl_2$, 1 $MgCl_2$, 9.4 Mg-ATP, 0.5 Na-GTP, 5.0 EGTA, 10 HEPES. Pipette resistance was between 10–15 MΩ. In some experiments, we increased the pH to 9.2 by adding NaOH. Cone PRs and HCs were voltage-clamped using an Axopatch 200B patch clamp amplifier (Axon Instruments, Molecular Devices, Sunnyvale, CA, USA) and Alembic VE-2 amplifier (Alembic Instruments, Montreal, Quebec, Canada), respectively. Whole-cell currents were digitized with an Axon Digidata 1440A interface and acquired using Clampex 10.2.0.12 software. A measured liquid-junction potential of -9 mV was not corrected for in these experiments.

Cones and HCs were identified by their morphology and physiological properties (Van Hook & Thoreson, 2013). Charging curves for cones (n = 15) yielded the following passive parameters: membrane capacitance (C_m) = 76.1 1 ± 6.68 pF, access resistance (R_{access}) = 25.7 ± 2.86, membrane resistance (R_m) = 229.9 ± 53.3 MΩ, and time constant (τ) = 1.48 ± 0.07 ms. For HCs (n = 15): C_m = 41.9 ± 4.42 pF, R_{access} = 36.0 ± 2.87 MΩ, R_m = 239.4 ± 75.9 MΩ, and τ = 1.03 ± 0.11 ms.

Center-surround antagonistic stimulation

For the flatmount preparation, we obtained whole cell voltage-clamp recordings from cone PRs. Cones were held at -70 mV and stepped to different test potentials (-60, -50, -40, -35, -30, -25, -20, -15, and -10 mV) to activate I_{Ca} by different amounts. A spot plus annulus sequence was created in Microsoft Powerpoint and projected onto the

retina through a prism in the condenser pathway from a compact LED projector (MPro110; 3M Maplewood, MN, USA). The cone was first illuminated with small spot of light (diameter = 45 μm) for 1.5 s and then the surround was illuminated with an annulus (i.d. = 45 μm; o.d. = 1 mm) for another 1.5 s. The onset and offset of light were detected with a photodiode. Annular illumination sometimes evoked direct light response due to light scatter into the receptive field center of the cone. In each cell, we therefore subtracted the average amplitude of currents evoked at annulus onset and offset when the cone was held at -50 and -60 mV.

Paired recordings

For slice recordings, we obtained whole cell recordings simultaneously from both an HC and cone. Pairs of cells were determined to have a synaptic connection by stimulating the cone with a step pulse (from -70 to -10 mV, 50 ms) and observing if the simultaneously voltage-clamped HC (V_m = -60 mV) responded with a post-synaptic current. To assess feedback, the HC was stepped to one of four test potentials (-90, -60, -30, or 0 mV) for 1.9 s and then we measured the cone I_{Ca} with a ramp-voltage protocol (-90 to +60 mV, 0.5 mV/ms). Two sets of steps were given to each pair with a 45 s rest period between trials. In one set, the sequence of steps applied to the HC began with -90 mV and in the other set, the sequence began with 0 mV.

We evaluated the strength of HC to cone feedback by determining the changes in the peak amplitude (I_{peak}) of the cone I_{Ca} and the voltage at which the I_{Ca} is half maximal (V_{50}) (Cadetti & Thoreson, 2006). The I_{peak} was normalized as a percentage change compared to the I_{peak} values obtained when the HC was hyperpolarized to -90 mV. Changes in voltage-dependence were measured as the difference in V_{50} relative to the V_{50} measured when the HC was held at -90 mV.

Data were analyzed using Clampfit (Axon Instruments) or GraphPad Prism 4. Statistical significance was evaluated with a paired t-test with $P<0.05$ unless otherwise noted. All variability is reported as SEM.

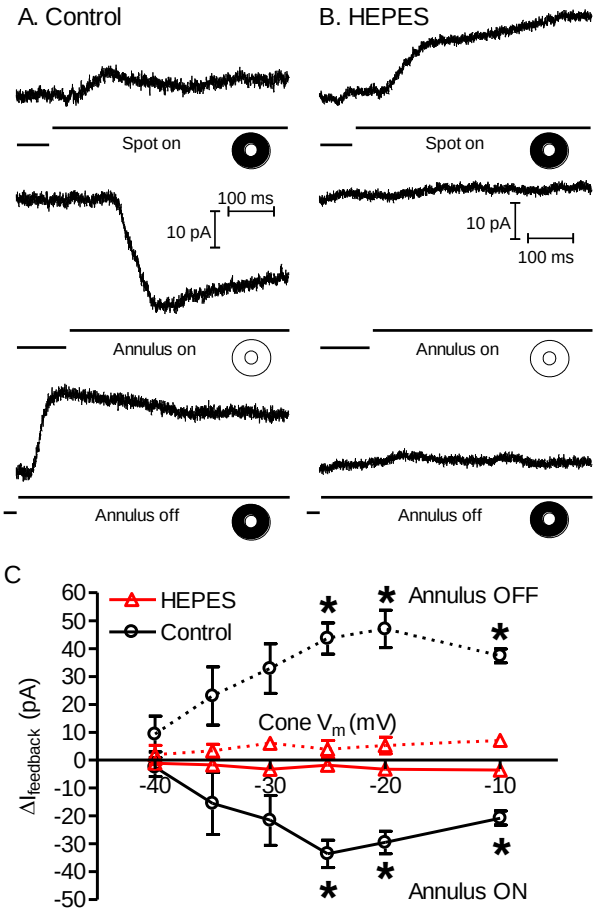

Figure 1. Center-surround antagonistic stimulation.

(A) A representative set of traces from a voltage clamped cone in a flatmount retina. Illumination of the cone with a spot of light evoked an $I_{outward}$ (top trace). Superposition of annular illumination evoked an inward $I_{feedback}$ (middle trace). Removal of the annulus caused an $I_{outward}$ reflecting loss of $I_{feedback}$ (bottom trace). **(B)** Same protocol with 10 mM HEPES buffer added to bath solution. Application of HEPES caused a slight increase in the light response due to blockade of inward $I_{feedback}$ (top trace). No currents were observed at onset (middle trace) and offset (bottom trace) of annular illumination showing that $I_{feedback}$ was eliminated by buffering synaptic pH change with HEPES. **(C)** Change in amplitude of feedback ($\Delta I_{feedback}$) upon onset and offset of annular illumination plotted against the cone membrane potential (V_m, N = 5). *Differences in $\Delta I_{feedback}$ between control and 10 mM HEPES achieved statistical significance at cone potentials of -25, -20 and -10 mV upon light on- and offset (Annulus ON: cone V_m = -25 mV P = 0.0063, -20 mV P = 0.0092, -10 mV P = 0.0077; Annulus OFF: cone V_m = -25 mV P = 0.0417, -20 mV P = 0.0367, -10 mV P = 0.0151).

2.3 Results

Carbonic anhydrase (CA)

Figure 1 (A – C) illustrates measurements of $I_{feedback}$ from a cone in flatmount retina. In this example, the cone was voltage clamped at -30 mV which is near the V_{50} value for I_{Ca}. Application of a bright spot of light onto this cone evoked an outward light-evoked current ($I_{outward}$). We then applied an annulus to illuminate the surrounding region of retina while maintaining central

illumination to limit activation of the cone by light scattered back into the center. This annular or surround illumination evoked an inward current ($I_{feedback}$) due to an increase in I_{Ca} resulting from release of negative HC feedback. Removal of annular illumination caused a decrease in $I_{feedback}$ (Fig. 1A). We repeated this sequence of illumination while holding the cone at different potentials from -60 to -10 mV. The increase in $I_{feedback}$ evoked by annular illumination and decrease evoked by its cessation show a voltage-dependence that parallels I_{Ca} activation with a threshold above -50 mV and peak near -25 mV (Fig. 1C).

One possible source of extracellular protons in the synaptic cleft is the activity of extracellular CA which catalyzes the conversion of CO_2 and H_2O into H_2CO_3, which then spontaneously dissociates into H^+ and HCO_3^- . While CA can be expressed both intra- and extracellularly (Sarthy & Ripps, 2001), extracellular CA XIV has been observed in the outer plexiform layer (OPL) of goldfish and mouse retina (Nagelhus *et al*., 2005; Fahrenfort *et al*., 2009). Using the flatmount retina preparation, we tested whether antagonizing extracellular CA function had any effect on HC feedback currents by bath applying benzothiophene-3-ylmethylsulfamide (FC5-207a; 1 μM), a membrane-impermeant CA antagonist (Winum *et al*., 2007; Fiaschi *et al*., 2013). Consistent with extracellular alkalinization resulting from inhibition of extracellular carbonic anhydrase, FC5-207a caused a negative shift in activation potential for I_{Ca} and an increase in I_{peak} (Fig. 2A; N = 7). For comparison, we also show the effect of alkalinization from 7.4 to 7.8 on I_{Ca} in Fig. 2B. However, as shown in Fig. 2C, we observed no significant difference in $I_{feedback}$ evoked at onset or offset of surround illumination.

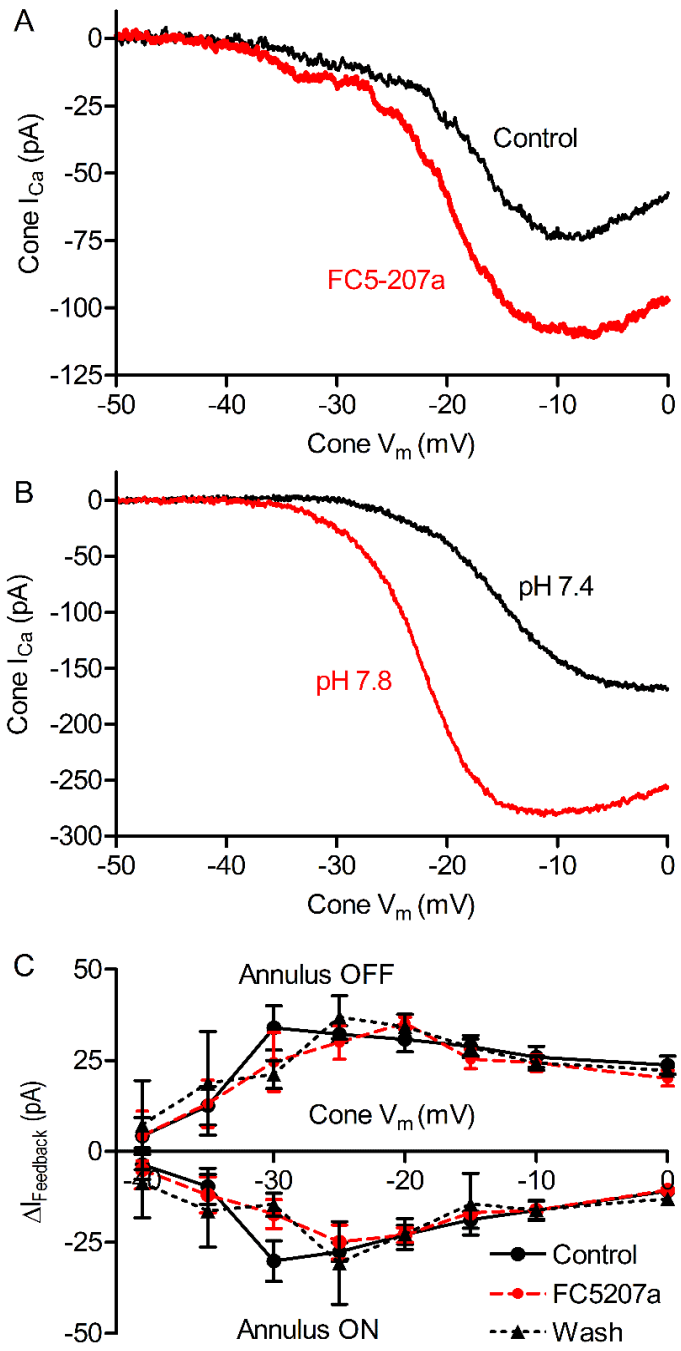

Figure 2. Extracellular carbonic anhydrase (CA) does not contribute protons for feedback.

(A) Effect of membrane-impermeant CA antagonist FC5-207a (1 μM) on I_{Ca}. Application of FC5-207a shifted the activation threshold of I_{Ca} to more negative potentials along and increased the peak current (I_{peak}). This is similar to extracellular alkalinization (n = 7) as shown in **(B)** where the extracellular solution was changed from pH 7.4 to 7.8. **(C)** $I_{feedback}$ was unchanged by application of 1 μM FC5-207a (N = 7).

Paired recording protocol

Because many of the drugs tested in later experiments could potentially influence light responses of cones or HCs, we used a different approach to test feedback in which we directly manipulated the membrane potential of a voltage-clamped HC while recording I_{Ca} in a simultaneously voltage-clamped cone. As illustrated in Fig. 3, we stepped the HC to 4 different potentials (-90, -60, -30, and 0 mV) and then measured I_{Ca} by applying a ramp voltage protocol (-90 to +60 mV, 0.5 mV/ms) to the cone. We confirmed synaptic connectivity between the HC and cone by the presence of a post-synaptic current in the HC during depolarizing stimulation of the cone. For example, Fig. 3A shows the inward synaptic currents (arrow) evoked by activation of I_{Ca} during the voltage ramp applied to the cone (Fig. 3B). The ramp-evoked cone currents were leak subtracted and plotted against the cone holding potential (Fig. 3C). As shown in this example, progressively depolarizing the HC membrane potential caused cone I_{Ca} to activate at more positive potentials and attain a smaller peak current. To assess the strength of HC feedback, we plotted the change in membrane potential at which the current was half maximal (V_{50}; Fig. 3D) and the change in peak amplitude (Fig. 3E) against the HC holding potential. We normalized data from different cells by measuring changes in I_{Ca} amplitude and activation relative to values determined when the HC was voltage-clamped at -90 mV.

Vesicular Protons

Synaptic vesicles utilize a vesicular ATPase (V-ATPase) to take up protons and use the proton gradient to load anionic neurotransmitters (Poudel & Bai, 2014). V-ATPase activity produces a luminal vesicle pH of 5-6 (Liu & Edwards, 1997). Fusion of glutamate-filled vesicles in cone terminals releases protons into the synaptic cleft where they can have an inhibitory effect on presynaptic I_{Ca} (DeVries, 2001). HCs contain acidic

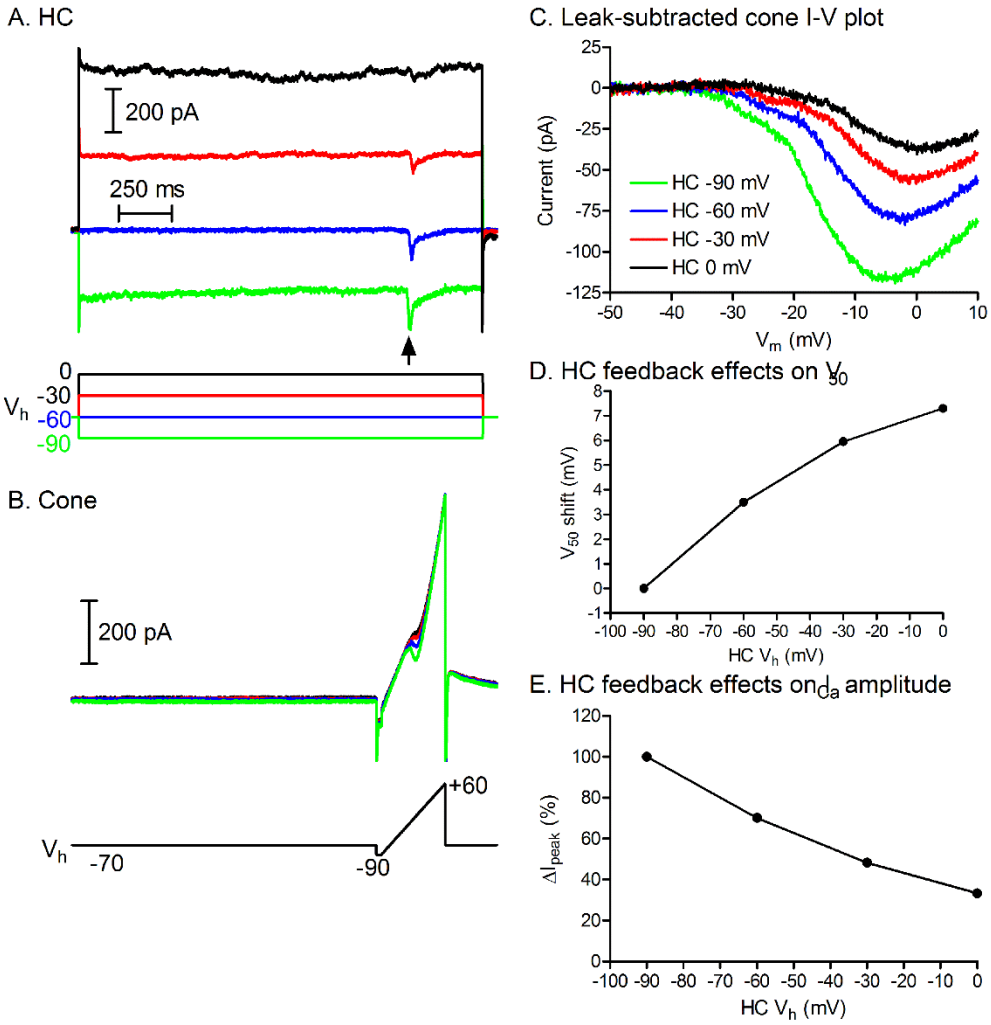

Figure 3. Protocol for measuring feedback with paired recordings.

(A) Currents in an HC during steps from -60 mV to -90 (green), -60 (blue), -30 (red) and 0 mV (black). Note the inward synaptic currents evoked by activation of I_{Ca} in the cone by the ramp voltage protocol (arrow). (B) Currents recorded simultaneously in a cone during application of a voltage ramp while the HC was stepped to different potentials. (C) Leak-subtracted I_{Ca} vs. cone holding potential shows an increase in I_{peak} and shift in activation of I_{Ca} to more negative potentials as the HC was hyperpolarized. (D) Feedback-induced changes in activation (V_{50}) as a function of changes in HC holding potential. V_{50} was measured as the cone V_m at which the I_{peak} was half-maximal. All values were then normalized to the V_{50} measured when the HC V_m = -90 mV. (E) Change in I_{peak} as a function of HC holding potential. Data are plotted as the percentage decrease in I_{peak} from that measured when HC V_m = -90 mV. All data from the same cell pair.

GABA-laden synaptic vesicles at their terminals (Lee & Brecha, 2010). The continuous release of glutamate or GABA into the synaptic cleft in darkness could thus potentially provide a tonic source of protons.

To test this hypothesis, we blocked V-ATPases by incubating retinas in 3.5 μM bafilomycin (plus 1% BSA in amphibian superfusate) for 12 hrs and then assessed the strength of feedback using our paired-recording protocol (Fig. 3). We also continuously applied bafilomycin during the recordings. Consistent with block of V-ATPase activity, bafilomycin treatment completely eliminated HC light responses, miniature EPSCs in HCs, and EPSCs evoked by depolarizing stimulation of presynaptic cones in paired recordings. Because it blocked HC responses, bafilomycin also eliminated $I_{feedback}$ evoked by surround illumination in the flatmount preparation. However, with our paired recording protocol, the changes in I_{peak} and V_{50} induced by changes in HC holding potential were not eliminated by bafilomycin. Fig. 4 shows a series of I_{Ca} measurements made at different HC holding potentials. As in control untreated cells, there was a marked rightward shift in activation and decrease in peak amplitude of cone I_{Ca} with HC depolarization. Fig. 4A and B show that the changes in I_{peak} and V_{50} values did not differ significantly between bafilomycin-treated tissue and control retinas that were incubated overnight in BSA-containing amphibian superfusate without bafilomycin. Thus, vesicular protons released from either cone or HCs are not required for lateral-inhibitory feedback from HCs to cones. These data also show that the release of glutamate from the cone terminal is not required for feedback.

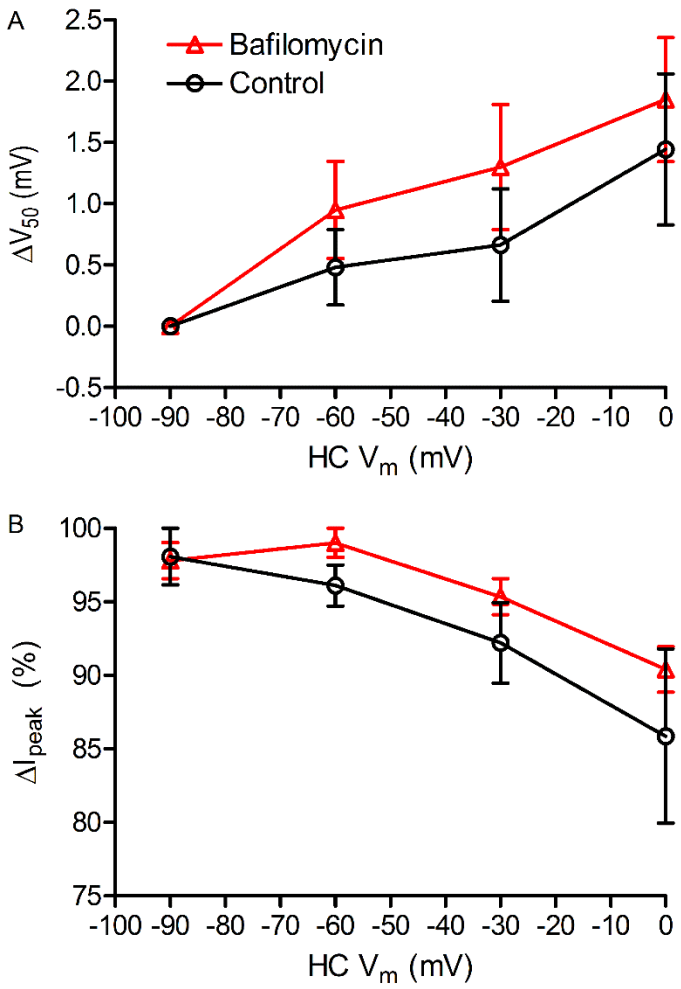

Figure 4. Vesicular protons do not mediate feedback from HCs to cone PRs.

(A) The shift in V_{50} and **(B)** the percentage change in the I_{peak} the between control and bafilomycin-treated retinas plotted against the HC membrane potential. After incubating retinas in 3.5 µM bafilomycin for 12 hrs (N = 3), the change in V_{50} and I_{peak} caused by changes in HC membrane potential were not significantly different from controls (N = 4). Both **(A & B)** were plotted relative to values when HC V_m = -90 mV.

NHEs

The extrusion of protons by NHEs contributes to maintenance of the acidic internal pH of ~7.2 primarily in PRs and HCs (Koskelainen *et al*., 1993; Saarikoski, 1997; Kalamkarov, 1996; Haugh-Scheidt & Ripps, 1998). To test whether NHEs might provide a source of extracellular protons at the cone synapse, we eliminated the inward Na^+

driving force by replacing extracellular Na^+ with choline. Na^+ replacement eliminated the feedback-induced changes in both I_{peak} and V_{50} of cone I_{Ca} caused by changes in HC holding potential (Fig. 5). The effect on V_{50} was statistically significant at the HC holding potential of 0 mV and the effect on I_{peak} was statistically significant at HC holding potentials of -30 and 0 mV. Feedback-induced changes in I_{peak} and V_{50} both recovered after returning to the control superfusate. These data indicate that feedback requires an inward gradient for Na^+.

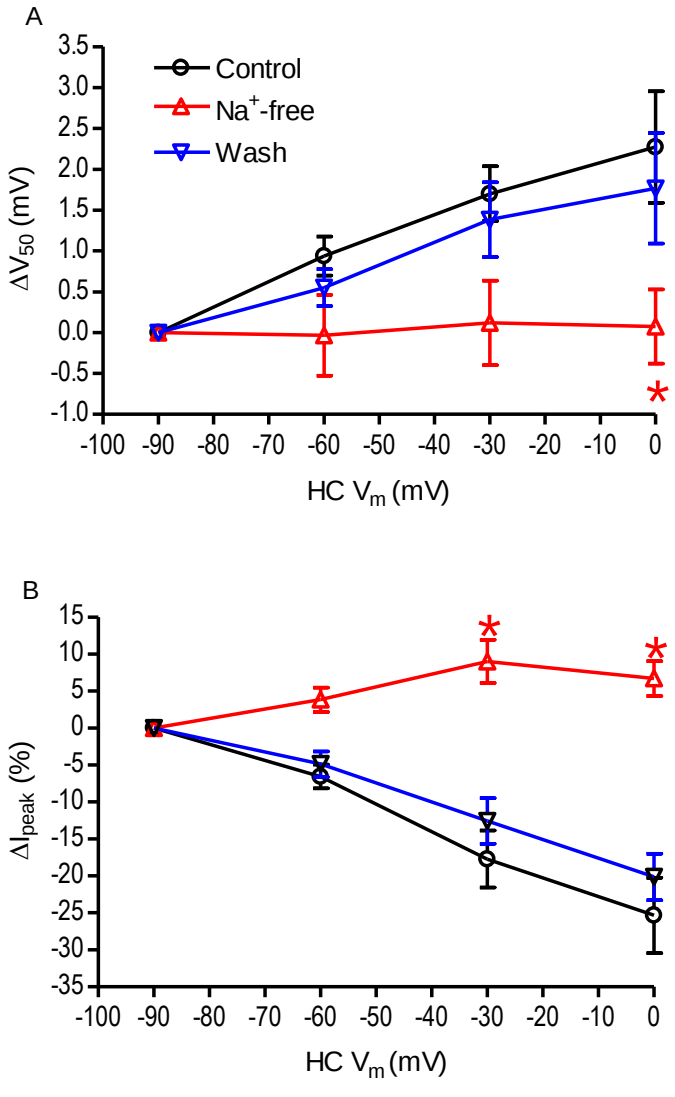

Figure 5. Removal of extracellular Na^+ and alkalinizing the intracellular milieu of HC eliminated feedback.

(A & B) When Na^+ in the extracellular solution was replaced with choline the feedback-induced shift in the V_{50} and changes in the I_{peak} were eliminated. (N = 5; V_{50}: HC V_m = -30 mV, P = 0.052, paired t-test between test and control; 0 mV, P = 0.043; I_{peak}: HC V_m = -60 mV, P = 0.059, -30 mV, P = 0.020; 0 mV, P = 0.020) Both recovered after washout. * indicates statistical significance.

To determine whether HCs or cones provided the major source of protons, we then tested effects on HC to cone feedback of reducing the intracellular proton concentration to restrict the availability of protons needed for NHE activity. To do so, we obtained paired recordings and introduced an alkaline patch pipette solution with pH 9.2 into either the cone or HC. We compared the changes in V_{50} and amplitude with controls recordings obtained using the normal pH 7.2 pipette solution. The feedback-induced differences relative to measurements at -90 mV in both V_{50} and I_{peak} were significantly reduced (n = 7) at HC holding potentials of -60, -30 and 0 mV by introducing pH 9.2 solution into the HC (Fig. 6). HCs retained their viability as evidenced by the fact that their holding currents were unchanged throughout the recordings. In contrast, feedback-induced differences in V_{50} were not altered by alkalinization of the cone cytosol (Fig. 6; n = 4). However, changes in I_{peak} were abolished by alkalinization of the cone cytosol. This probably does not reflect a true loss of feedback since changes in V_{50} were not changed. The site at which protons modulate channel conductance resides within the pore (Chen & Tsien, 1997) and so it is possible that alkalinization of the cone interior may overwhelm the ability of extracellular changes to alter pH within the pore. These results support the idea that extrusion of protons by NHE could provide a source of extracellular protons and show that the protons are likely to be derived from HC cytosol.

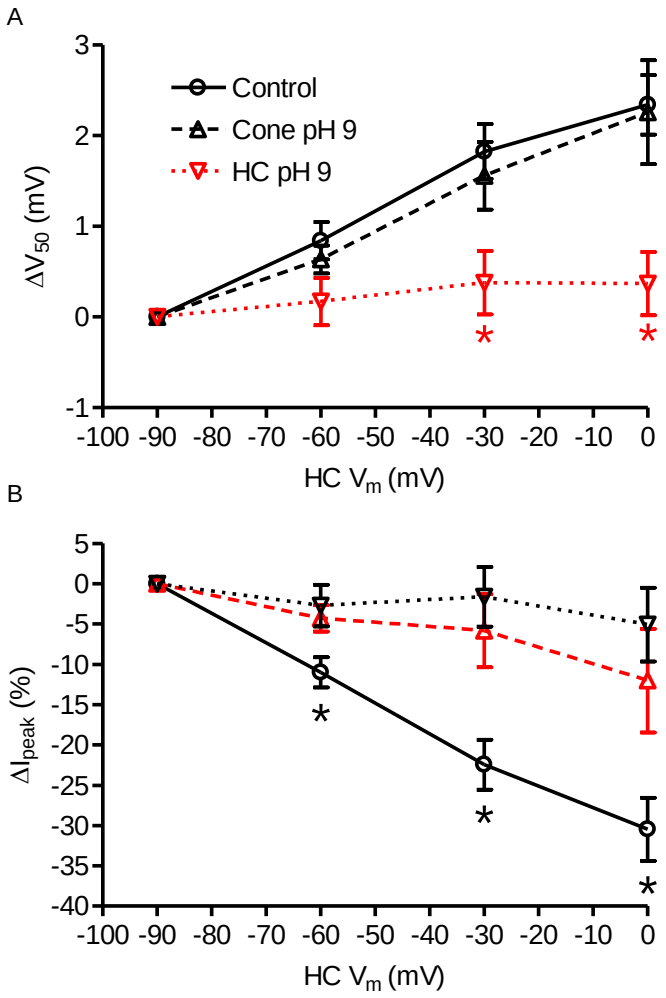

Figure 6. Effects of alkalinizing cone and HC cytosol on feedback during paired recordings.

Either the cone or HC pipette solution was buffered to ~pH 9.2 and feedback was assessed using the paired recording protocol. **(A)** Alkalinizing HC cytosol (N = 7) eliminated the feedback-induced shift in V_{50} with respect to control (N = 22; unpaired t-test, ΔV_{50}: HC V_m = -60 mV, P = 0.0403; -30 mV, P = 0.0072; 0 mV, P = 0.0035). Alkalinizing cone cytosol (N =4) did not alter the feedback-induced shift in V_{50}. (B) Alkalinizing HC and cone cytosol both caused a significant reduction in feedback-induced effects on I_{peak} compared to control (HC alkalinization: HC, V_m = -60 mV, P = 0.0233, unpaired t-test; -30 mV P = 0.0009, 0 mV P = 0.0013; cone alkalinization: V_m = -30 mV, P = 0.0163; 0 mV, P = 0.0357).

Vessey *et al*. (2005) showed that an NHE antagonist, amiloride, interfered with feedback, but amiloride is also known to interact with a variety of channels including

epithelium sodium channels (ENaC), acid-sensing ion channels (ASIC), and TRP channels. To further test the idea that a NHE may be involved in feedback, we tested the NHE antagonists (Masereel *et al*., 2003) cariporide (N-(Aminoiminomethyl)-5-cyclopropyl-1-(5-quinolinyl)-1H-pyrazole-4-carboxamide) and zoniporide (N-(Diaminomethylidene)-3-methanesulfonyl-4-(propan-2-yl)benzamide) on feedback. Cariporide (10 μM) caused a significant reduction in feedback-induced changes in I_{peak} (N = 7 cone/HC pairs, paired comparisons at -60 and -30 mV, $p < 0.05$) and V_{50} (paired comparison at -30 mV, $p < 0.05$; Fig 7A & B). The effects of this drug did not show recovery during washout period. Application of zoniporide (25 μM; N=5) showed a similar trend towards a reduction in the change of I_{peak} and V_{50} values but did not attain statistical significance.

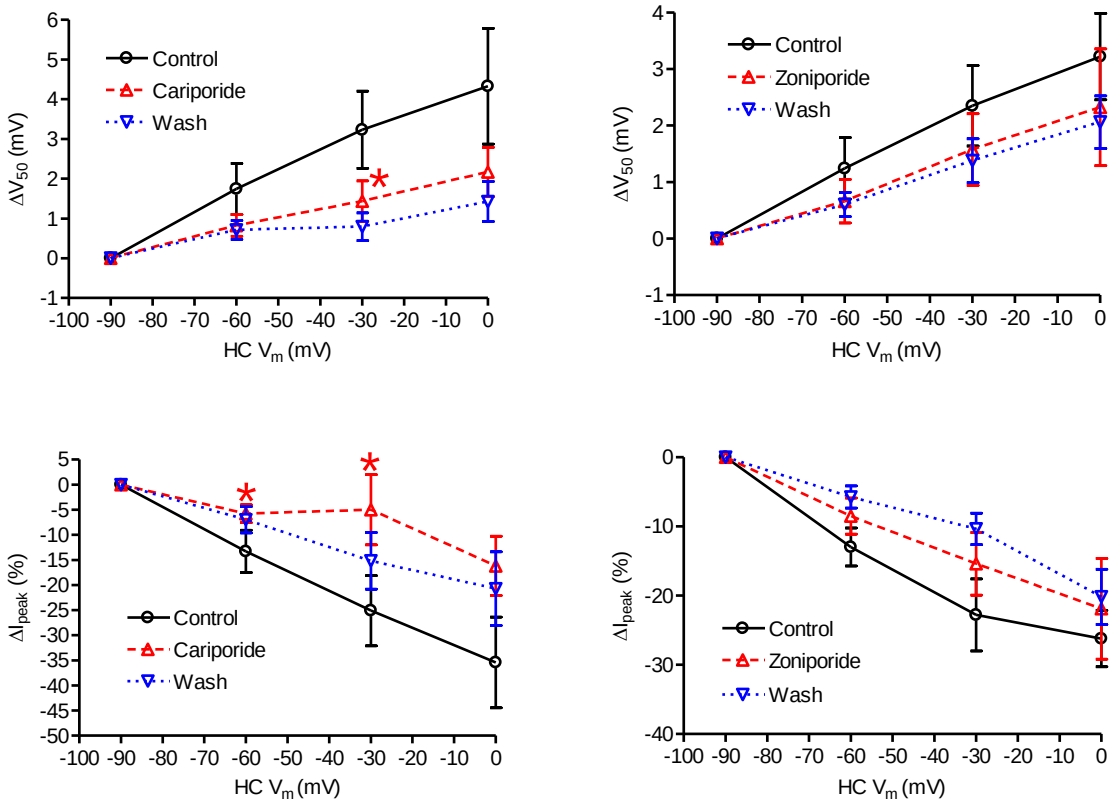

Figure 7. The NHE antagonist, cariporide, reduced feedback.

(A & B) Cariporide (N = 7) caused a significant reduction in feedback-induced changes in V_{50} **(A)** and I_{peak} **(B)** (V_{50}: HC V_m = -60 mV, P = 0.0631, paired t-test; -30 mV, P = 0.0356; 0 mV, P = 0.0880; I_{peak}: HC V_m = -60 mV, P = 0.0408; -30 mV, P = 0.0230; 0 mV, P = 0.0599). **(C & D)** There was a similar trend towards a reduction in feedback strength with zoniporide (25 mM) but the differences did not attain significance. Neither group recovered from application of the drug.

We tested whether feedback was sensitive to changes in the extracellular pH by obtaining paired recordings in the control-pH 7.4 solution and then switching to a solution with either pH 7.1 or 7.8. These solutions were prepared by using 12 or 32 mM $NaHCO_3$ rather than 22 mM as used in the control solution. As shown in Fig. 8, HC feedback as measured by decreases in both I_{peak} ($P < 0.015$, one-way ANOVA at HC V_m = -60, -30, & 0 mV) and V_{50} shifts ($P < 0.05$, one-way ANOVA at HC V_m = 0 mV) was significantly strengthened by extracellular acidification suggesting that changes in the trans-membrane concentration gradient for protons or bicarbonate alter feedback strength.

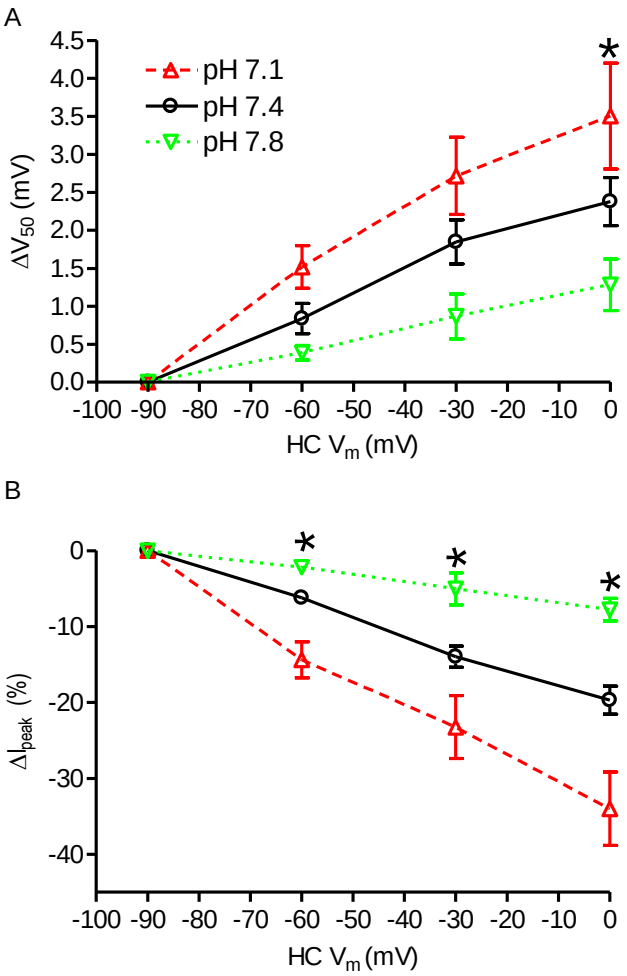

Figure 8. Strength of feedback increases as extracellular solution becomes acidified.

Using the paired recording protocol, feedback was tested at pH 7.8 (N = 5), 7.4 (N = 23), or 7.1 (N = 7) in the bicarbonate-buffered ringer solution. **(A)** There was an increase in the V_{50} shift as the external pH was lowered (one-way ANOVA, V_{50}: HC V_m = -60 mV, P = 0.0615; -30 mV, P = 0.0504; 0 mV, P = 0.0402). **(B)** There was also an increase in the change in the I_{peak} as the external pH was lowered (one-way ANOVA, I_{peak}: HC V_m = -60 mV, P = 0.0001; -30 mV P = 0.0025; 0 mV, P = 0.0003).

The sensitivity of feedback to changes in pH could be due to changes in either the proton or reflect changes in the bicarbonate gradients. Using the paired recording protocol, we looked at effects of removing bicarbonate on feedback. We began by adding 1 mM HEPES to our normal saline solution to increase the buffering capacity slightly. This produced a decrease in the changes in the V_{50} and amplitude (Fig. 8A; P

< 0.05, unpaired Student's t-test at HC V_m = -30 & 0 mV). We then removed bicarbonate, leaving 1 mM HEPES to maintain a constant pH of 7.4, and saw that feedback was abolished (Fig. 8B; P < 0.05, unpaired Student's t-test comparing V_{50} and amplitude for HEPES alone to bicarbonate plus HEPES at HC V_m = -30, & 0 mV). We then tested whether sodium-bicarbonate cotransporters (NBCs) might be involved in feedback by using a bicarbonate transport inhibitor (Romero *et al*., 1997; Romero *et al*., 2013), 4,4′-diisothiocyano-2,2′-stilbene-disulfonic acid (DIDS) (Virkki *et al*., 2002; Shmukler *et al*., 2014). DIDS significantly reduced feedback-induced changes in V_{50} and I_{peak} of the cone I_{Ca} in paired recordings (N = 7) at a concentration of 500 µM (N = 5; Fig. 9C & D; P < 0.05, unpaired Student's t-test at HC V_m = -60 mV, -30, & 0 mV). Effects of DIDS were not significant at a concentration of 100 µM. These data suggest that an NBC and/or a Na^+-dependent bicarbonate/Cl^- exchanger are involved in mediating lateral-inhibitory feedback from HCs to cones.

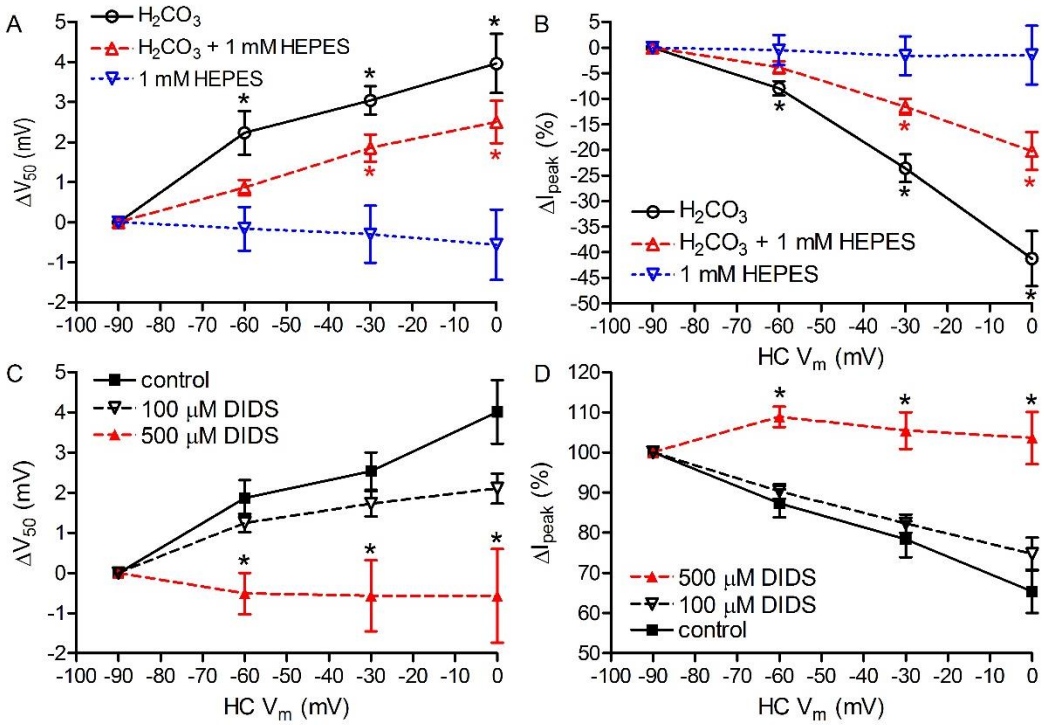

Figure 9. Bicarbonate is required for feedback and inhibition of anion transport mechanisms by DIDS blocked feedback. (A) A slight increase in buffering capacity of the external solution by addition of 1 mM HEPES decreased in the magnitude of the activation shift in V_{50} (unpaired Student's t-test, control (N = 5) vs. $NaHCO_3$ + 1 mM HEPES (N = 8), ΔV_{50}: HC V_m = -30 mV, P = 0.0406; 0 mV, P = 0.0458), while removal of bicarbonate eliminated the shift (unpaired Student's t-test, control vs. 1 mM HEPES (N = 5) only, V_{50}: HC V_m = -60 mV, P = 0.0253; -30 mV, P = 0.0050; 0 mV, P = 0.0042; $NaHCO_3$ + 1 mM HEPES vs. 1 mM HEPES only, -30 mV, P = 0.0451; 0 mV, P = 0.0266) **(B)** Feedback-induced changes in I_{peak} were reduced when 1 mM HEPES was added to the normal solution (unpaired Student's t-test, control vs. $NaHCO_3$ + 1 mM HEPES, I_{peak}: HC V_m = -30 mV, P = 0.0078; 0 mV, P = 0.0045) and abolished when bicarbonate was removed (unpaired Student's t-test, $NaHCO_3$ + 1 mM HEPES vs. control, I_{peak}: HC V_m = -60 mV, P = 0.0521; -30 mV, P = 0.0037; 0 mV, P = 0.001; $NaHCO_3$ + 1 mM HEPES vs. 1 mM HEPES only, -30 mV, P = 0.0027; 0 mV, P = 0.0373). **(C & D)** Application of the anion transport inhibitor DIDS (500 µM, N=5) significantly inhibited feedback-induced changes in V_{50} **(C)** and I_{peak} **(D)** (unpaired Student's t-test, df=15; V_{50}: HC V_m = -60 mV, P = 0.0080; -30 mV, P = 0.0039; 0 mV, P = 0.0063; I_{peak}: HC V_m = -60 mV, P = 0.0019; -30 mV, P = 0.0029; 0 mV, P = 0.0011). Using a lower concentration of DIDS (100 µM; N = 7) produced a weaker effect that did not attain statistical significance.

Analysis of the Kinetics of Feedback

It has been proposed that a purely electrical ephaptic mechanism may contribute to negative feedback from HCs to cone PRs (Byzov & Shura-Bura, 1986; Kamermans *et al*., 2001; Kemmler *et al*., 2014). Ephaptic voltage changes should occur instantaneously. We therefore measured the kinetics of feedback currents in cones evoked by voltage steps applied to simultaneously voltage-clamped HCs. Our experimental approach is illustrated in Figure 10 which shows data averaged from two trials in the same cell. We repeated trials 2-4 times in each cell. During each trial, we stepped the HC from -60 to -30 mV for 2 s to simulate a period of darkness and then hyperpolarized the HC to -90 mV for 0.5 s to simulate a bright light flash. During the trial, we depolarized the cone to either -30 or -20 mV to partially activate I_{Ca}. As shown earlier, hyperpolarizing the HC membrane potential enhances I_{Ca} by increasing the peak amplitude and shifting its activation to more negative potentials. The increase in I_{Ca}

caused by HC hyperpolarization of the HC therefore increased I_{Ca} resulted in an inward feedback current (Fig. 10B & C, arrow). Fig. 10C shows the change in feedback current from the same cell at a higher gain and faster time base. The feedback-induced increase in I_{Ca} was fit better with two exponentials than with a single exponential. The contribution of the slow component varied from cell to cell but we observed a clear second component in 12/13 cell pairs (cone V_m = -30 mV). This second component had an average time constant of τ_{slow} = 530 ± 111 ms (N = 12). To measure the initial fast kinetics of feedback as accurately as possible, we fit the first 50-100 ms with a single exponential (Fig. 11C). We chose the fitting region that gave the best fit to the initial change in feedback current. When the cone was voltage clamped at -30 mV, the inward feedback current evoked by the hyperpolarizing voltage step applied to the HC averaged -3.2 ± 0.83 pA in amplitude and showed an onset that could be fit with a single exponential time constant, τ_{fast}, averaging 14.2 ± 1.8 ms (N = 8). We also tested a few cones held at -20 mV to activate I_{Ca} more strongly. In these cells, the feedback current was -4.26 ± 1.8 pA and τ_{fast} averaged 12.5 ± 0.9 ms (N = 7). We never observed an instantaneous inward current at the beginning of the HC hyperpolarizing voltage step.

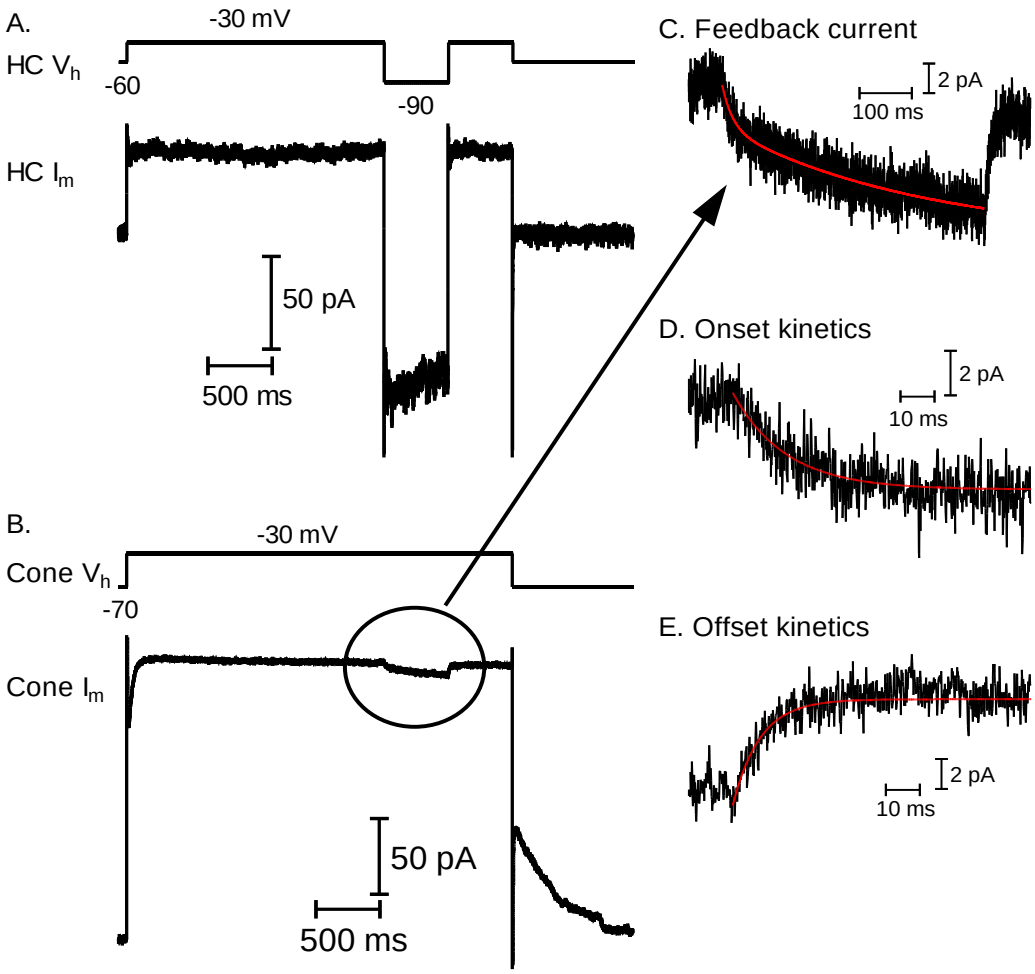

Figure 10. Testing for an ephaptic connection: protocol and feedback currents.

(A) The step waveform applied to the voltage-clamped HC (top). HC membrane current (bottom, I_m). **(B)** Voltage protocol in the cone (top). Simultaneously recorded cone membrane current (bottom, I_m). **(C)** Expanded view of $I_{feedback}$ in the same cone fit with a double-exponential curve. **(D & E)** Single exponential fits to the onset **(E)** and offset **(F)** of $I_{feedback}$ accompanying onset and offset of the step from -30 to -90 mV in the HC while the cone was voltage clamped at -30 mV.

We also measured the kinetics of the offset of the feedback current in cones when the HC voltage returned from -90 to -30 mV. We found a fast time constant at offset of the step averaging 13.6 ± 0.8 ms (cone V_m = -20 mV) and 14.5 ± 1.4 ms (cone V_m = -30 mV) similar to the time constants at the onset of feedback. A clear slow component was less consistently evident at offset of the HC hyperpolarizing voltage

step.

The measurement resolution in these experiments is limited by the summed voltage clamp speeds of the cone and HC membranes. We assessed voltage clamp speed from the membrane charging curves. Cone and HC charging curves could both be fit by single exponentials (Fig. 11A-B). For trials in which the cone was voltage clamped at -30 mV, the charging time constants averaged 2.76 $\pm$ 0.3 ms (N = 8) and 1.06 $\pm$ 0.1 ms (N = 8) for the HC. For trials in which the cone was voltage clamped at -20 mV, the time constants averaging 1.80 $\pm$ 0.4 ms (N = 7) for the cone and 0.95 $\pm$ 0.2 ms (N = 7) for the HC. When summed together for each cell pair, $\tau_{cone} + \tau_{HC}$ for was 3.44 $\pm$ 0.4 ms for cone V_m = -30 mV trials and 2.75 $\pm$ 0.5 ms for cone V_m = -20 mV trials. As shown in the scatter plot in Fig. 11C, the measurement resolution ($\tau_{cone} + \tau_{HC}$) was significantly faster than the feedback time constants measured at both onset and offset of the hyperpolarizing voltage step applied to the HC. This was true whether the trials were conducted at a cone holding potential of -30 mV or at -20 mV. Lines connect the time resolution and feedback time constants in trials showing the fastest feedback time constants. The feedback currents at onset and offset of the HC voltage step were 9.8 - 11.1 ms slower than the combined voltage clamp speed of the two cells. This difference is considerably slower than the activation kinetics of I_{Ca} evoked by a step to -30 mV in salamander cones (τ = 3.1 $\pm$ 0.22 ms at -30 mV, Warren *et al*., unpublished). This indicates that feedback is not fast enough to be produced by ephaptic mechanism.

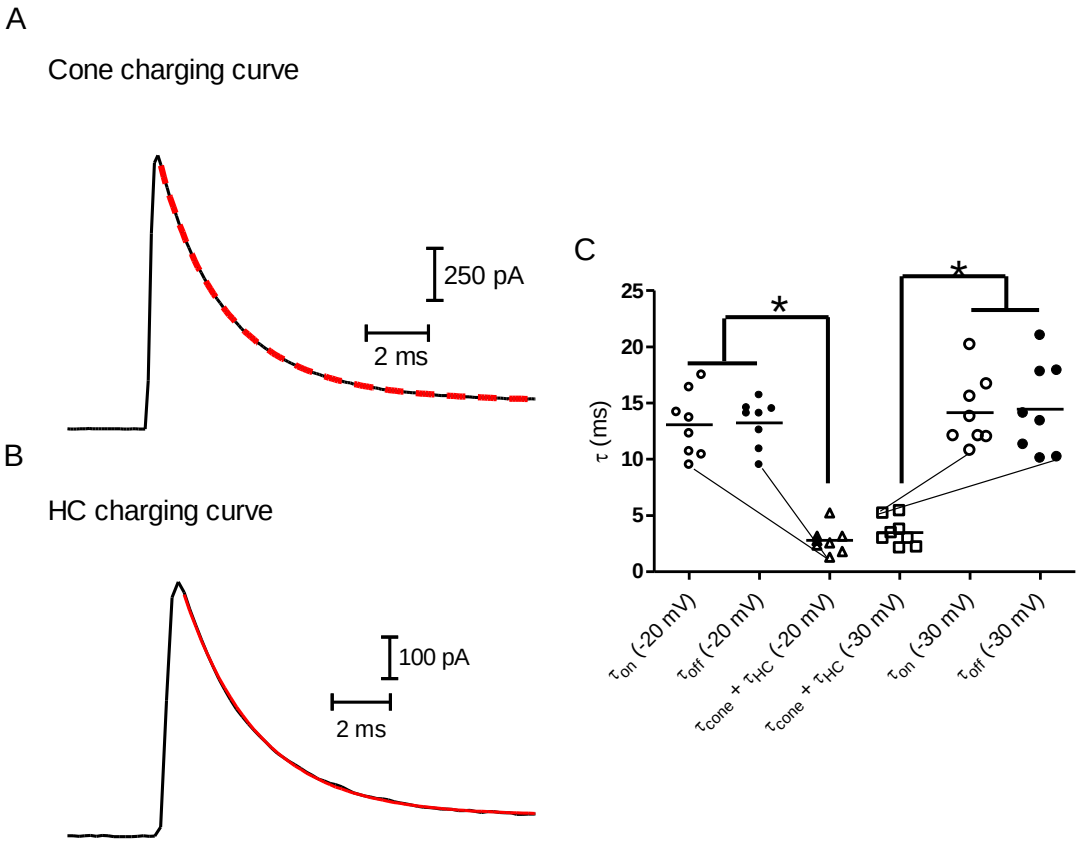

Figure 11. Comparing measurement time resolution with feedback speed.

(A & B) Capacitive currents evoked by voltage steps applied to a cone (top; -70 to -30 mV) and a HC (bottom; -60 to -30 mV). The charging curves were fit with a single-exponential functions to obtain the time constants (τ) for charging of the cell membrane (cone: 2.65 ms; HC: 1.27 ms). **(C)** Scatter plot showing the fast time constants of feedback currents at onset of the HC voltage step, τ_{on}, and offset of the step, τ_{off}, when the cone was held at -20 mV, τ_{on}, and offset of the step, τ_{off}, when the cone was held at -20 mV, τ_{on} and τ_{off} averaged 12.5 ± 0.9 ms and 13.6 ± 0.8 ms, (N = 8). When the cone was held at -30 mV, τ_{on} and τ_{off}, averaged 14.2 ± 1.1 and 14.5 ± 1.4 ms, respectively (N = 8). The time resolution for these recordings was limited by the sum of the charging time constants in the cone and HC. $\tau_{cone} + \tau_{HC}$ averaged 3.44 ± 0.4 ms for trials in which the cone V_m = -30 mV and 2.75 ± 0.5 ms for trials in which the cone V_m = -20 mV. Lines connect the time resolution and feedback time constants in trials showing the fastest feedback time constants. The differences between the feedback time constant (τ_{on} and τ_{off}) and the time resolution ($\tau_{cone} + \tau_{HC}$) were significantly different for all four comparisons (t-tests, paired comparisons; τ_{on}, -20 mV, $P < 0.0001$; τ_{on}, -30 mV, $P < 0.0001$; τ_{off}, -20 mV, $P < 0.0001$; τ_{off}, -30 mV, $P < 0.0002$).

2.4 Discussion

Sources of Protons

There are a number of different mechanisms that help to regulate pH within and around cells (Boron, 2004; Casey *et al*., 2010). However, only three mechanisms are known to be sources for extracellular protons: 1) protons liberated by the activity of extracellular carbonic anhydrase (Sarthy & Ripps, 2001; Fahrenfort *et al*., 2009; Vessey *et al*., 2005), 2) protons released by exocytosis of acidic vesicles (Chesler, 2003; DeVries, 2001), and 3) NHE (Koskelainen *et al*., 1993; Kalamkarov *et al*., 1996).

The CA inhibitors benzolamide and methazolamide have both been shown to interfere with feedback (Vessey *et al*., 2005; Fahrenfort *et al*., 2009). Although often touted as membrane-impermeant, benzolamide, like methazolamide, is actually membrane-permeant (Supuran & Scozzafava, 2004). To test for the role of extracellular CA, we therefore tested an improved membrane-impermeant CA inhibitor, FC5-207a. The compound caused changes in the activation and amplitude of I_{Ca} consistent with alkalinization of the synaptic cleft. However, it did not alter feedback indicating extracellular CA is not likely to be involved in the production of protons for feedback (Fig. 2A &B). The effects of benzolamide and methazolamide are likely due to their effects on intracellular CA activity. Consistent with this, Vessey *et al*. (2005) found that methazolamide only eliminated feedback effects induced by hyperpolarization of HCs by application of CNQX but not feedback effects of HC depolarization. They interpreted these findings as a reduction in the inward driving force for protons upon hyperpolarization. As methazolamide enters the cell, it causes an intracellular acidification and thus raises the cytosolic concentration of protons (i.e., a decrease in pH), thereby reducing the driving force of the proton into the HC upon hyperpolarization.

Our results also showed that vesicular protons are not involved in mediating

feedback. Incubating cells overnight in bafilomycin ensured that the drug would completely block proton transport into vesicles. In dissociated HCs from fish retina, Jouhou *et al*. (2007) used a pH-sensitive dye, 5-hexadecanoylaminofluorescein (HAF), to measure near-membrane pH changes and concluded that bafilomycin reduced extracellular acidification stimulated by HC depolarization. However, a subsequent study presented evidence that this dye reported near-membrane intracellular pH, not extracellular pH (Jacoby *et al*., 2014). Wang *et al*. (2014) found that bafilomycin blocked the ability of HC depolarization to acidify the synaptic cleft measured in transgenic zebrafish with a pH sensitive dye attached to the extracellular surface of cone Ca^{2+} channels (caliphluorin). While this might reflect species differences, variations in Wang *et al*.'s (2014) experimental preparation might account for the differences. Their experimental model does not directly test feedback per se, but could be influencing perisynaptic sources of protons (Wang *et al*., 2014)

Removal of Na^{+} from the extracellular medium eliminated feedback-induced changes in I_{Ca} and the NHE antagonist cariporide also significantly reduced feedback. These results indicate that the major source of protons involved in feedback is a NHE, consistent with the observation that amiloride, another NHE antagonist, blocks HC feedback to cones (Vessey *et al*., 2005). Our results suggest that the HC cytosol is the major source of protons extruded by NHE because reducing the proton concentration in HCs by use of a pipette solution with pH 9.2 also eliminated feedback-induced changes in cone I_{Ca}. Introducing pH 9.2 solution into cones did not alter the feedback-induced shifts in V_{50} suggesting that feedback remained intact. Alkalinizing the cone intracellular milieu did however abolish the changes in peak amplitude of cone I_{Ca} caused by changes in HC membrane potential. Ca^{2+} interacts with four key glutamate residues in the L-type Ca^{2+} channel pore as it passes into the cell (Chen *et al*., 1996). Protonation

of these residues interferes with this process. Alkalinizing the cytosol substantially may stabilize the protonation state, thereby decreasing the change in the I_{peak} when the HC is polarized. We could not eliminate the possibility that alkalinizing the HC intracellular milieu interfered with the removal of bicarbonate from the cell, however, in renal kidney cells bicarbonate transport is unaffected by changes in intracellular pH (Zhou *et al*., 2006).

We identified NHEs in HCs as the principal source of protons involved in feedback. However, NHEs are not voltage-dependent and so reduced NHE activity is unlikely be directly responsible for the cleft alkalinization caused by HC hyperpolarization (Demaurex *et al*., 1995; Fuster *et al*., 2004). We consider three other ways that HC hyperpolarization might reduce the free proton concentration in the cleft: 1) influx of protons into HCs through ion channels (e.g., through TRP channels, gap junction hemichannels or other proton permeable channels; Vessey *et al*. 2005; Wang *et al*., 2014); 2) efflux of bicarbonate buffer into the cleft (e.g., through bicarbonate exchange or GABA receptor anion channels, Liu *et al*. 2013); and 3) efflux of phosphate buffer into the cleft (e.g., by hydrolysis of ATP exiting HCs through pannexin channels; Vroman *et al*., 2014). We found that the strength of HC feedback increased with extracellular acidification from 7.8 to 7.4 to 7.1. The phosphate buffer created by hydrolysis of ATP has a $pK_a \approx 7.2$ and so Vroman *et al*. (2014) predicted that, contrary to our observations, acidifying the extracellular environment with pH 7.1 buffer should reduce feedback. To achieve stable pH values, we changed the bicarbonate concentration in our medium from 12 (pH 7.8) to 22 (pH 7.4) to 32 (pH 7.1) mM. Thus, our findings that feedback strength was increased by extracellular acidification are consistent with both an increased inward driving force for protons and greater outward driving force for bicarbonate with greater acidification. Using the expression data base from Siegert *et al*.

(2012) indicates that murine HCs express *Slc4a3* and *Slc4a5*. These transporters are blocked by DIDS. We found that DIDS at a concentration of 500 μM inhibited feedback. We also observed that removing or lowering the bicarbonate concentration from the external solution either eliminated or weakened feedback respectively. These two lines of evidence argue for either a NBC and/or a Na^+-dependent bicarbonate/Cl^- exchanger as a source of bicarbonate efflux or what the HC is using to alkalinize the cleft during HC hyperpolarization (Haugh-Scheidt & Ripps, 1998). Among the DIDS-sensitive *Slc4* family of bicarbonate transporters, the retinal gene expression database from Siegert *et al*. (2012) indicates that murine HCs express only *Slc4a3* and *Slc4a5*. *Slc4a5* is a sodium-bicarbonate transporter that has been shown be voltage-dependent, increasing HCO_3^- entry into cells upon depolarization (Virkki *et al*., 2002). This isoform shows punctate expression in the OPL (Kao *et al*., 2011) but low expression levels in photoreceptors (Siegert *et al*., 2012) suggesting that expression is concentrated in HC dendrites. *Slc4a5* knockout mice show a loss of photoreceptors and diminished electroretinogram a- and b-waves but feedback from HCs was not studied in these animals (Kao *et al*., 2011). *Slc4a3* is a Na^+-independent Cl^-/HCO_3^- exchanger. Unlike the concentrated expression of *Slc4a5* in HC dendrites, Slc4a3 is expressed throughout the entire HC (Kobayashi *et al*., 1994). There is also no evidence that *Slc4a3* activity is voltage-sensitive (Halligan *et al*., 1991) making it a less likely candidate for directly converting HC membrane potential changes into extracellular pH changes. However, feedback strength can be reduced by increases in cone Cl^- conductance (e.g., by activating GABA receptors or Ca^{2+}-activated Cl^- channels; Endeman *et al*., 2012) and these might involve secondary effects on Cl^-/HCO_3^- exchange. Liu *et al*. (2013) postulated a mechanism by which depolarization of HCs stimulates release of GABA which then acts in an autocrine fashion to activate HC GABA receptors. Reduced influx of bicarbonate through GABA receptor channels into the HC when it hyperpolarizes

causes the cleft to alkalinize (Liu *et al*., 2013). A number of studies have shown that GABA receptor antagonists do not block HC feedback to cones (Thoreson & Burkhardt, 1990; Verweij *et al*., 1996, 2003) suggesting that while GABA receptors may modify feedback under certain conditions (e.g., during certain circadian or illumination conditions), they are not the principal mechanism for feedback.

Kinetics of the $I_{feedback}$

Ephaptic voltage changes within the invaginating cone synapse induced by current flow into the HC should be instantaneous. Previous studies (Vroman *et al*., 2014; Kamermans *et al*., 2001) showed no difference between the kinetics of HC light responses and the kinetics of fast light-evoked feedback currents in cones. However, HC light response kinetics are intrinsically slow with a time to peak of ~100 ms. To overcome this limitation, we applied voltage steps directly to voltage-clamped HCs. However, even in a voltage-clamped HC, one cannot instantaneously change the membrane potential. The speed at which the applied voltage change is attained by the HC is reflected by the time course required for charging the HC membrane capacitance. The HC membrane charged with an average time constant of 1.06 ± 0.1 ms. The speed at which we can detect a change in feedback currents in the cone is also limited by the voltage clamp speed which had an average time constant of 2.75 ± 0.3 ms. Therefore, our measurement resolution was limited by an average of 3.81 ms. While an ephaptic voltage change should be instantaneous, a certain amount of time is nevertheless required for L-type Ca^{2+} channels to respond to a change in voltage within the synaptic cleft. The cone terminal contains CaV1.4 L-type Ca^{2+} channels (Morgans, 2001; Baumann *et al*., 2004). Baumann *et al*. (2004) found an activation time constant for heterologously-expressed mouse CaV1.4 channels to be around 0.6 ms when using a strong depolarizing step to fully activate the current. Corey *et al*. (1984) showed that

activation slowed with weaker depolarization finding activation time constants of ~8 ms at -30 mV and 3 ms at potentials above 0 mV (Corey et al., 1984). However, these experiments were conducted at 12ºC which would be expected to slow activation. At room temperature, Warren *et al*. (unpublished results) found that the activation time constant for L-type Ca^{2+} channels when stimulated with a step from -30 to -25 mV averaged 3.1 ± 0.22 ms. If we add in the time required for activation of L-type Ca^{2+} channels of 3.1 ms, this yields a total delay of 6.91 ms which is still well below the τ_{fast} = values of 12.5 ms obtained when cones were held at -20 mV and 14.2 ms when cone V_m = -20 mV. Thus, the feedback mechanism is not instantaneous but adds an additional delay. The kinetics of the feedback current are thus slower than predicted for an ephaptic mechanism, suggesting instead that the mechanism responsible for fast feedback is chemical.

Consistent with Vroman *et al*. (2014), we found that HC feedback to cones exhibited two kinetically distinct components. Earlier recordings of surround-evoked voltage changes in cones also revealed multiple components to feedback (Fuortes *et al*., 1973; O'Bryan, 1973). Different groups found different responses to surround elimination included sustained voltage changes and regenerative, spike-like responses arising from activation of I_{Ca} (Gerschenfeld & Piccolino, 1978, Piccolino & Gerschenfeld, 1980; Burkhardt *et al*., 1988). With regards to the initial onset kinetics of feedback, Vroman *et al*. (2014) points out, fast and slow components of feedback are useful for reducing spatial and temporal redundancies, respectively, in the visual input. Slow feedback can remove temporal redundancies whereas fast feedback allows spatially-averaged luminance to be constantly subtracted from local changes even when the visual scene changes rapidly. While we find that fast feedback is not instantaneous, it is still sufficiently fast to serve this purpose. A fast feedback mechanism with a time constant of

~8 ms is considerably faster than the slow kinetics of HC light responses and so it does not add noticeably to the speed at which feedback currents are induced in cones by surround illumination.

Appendix A: Abbreviations

List of Abbrevations

AMPA	alpha-amino-3-hydroxy-5-methyl-4-isoxazoleproprionic acid
BAF	Bafilomycin A1
BSA	Bovine Serum Albumin
BP	Bipolar cell
CA	Carbonic anhydrase
cariporide	N-(aminoiminomethyl)-5-cyclopropyl-1-(5-quinolinyl)-1H-pyrazole-4-carboxamide
cyclic GMP	Guanosine 3',5'-cyclic monophosphate
DIDS	4,4'-Diisothiocyano-2,2'-stilbenedisulfonic acid
EIPA	5-(N-ethyl-N-isopropyl)amiloride
E_{rev}	Reversal potential
FC5-207a	Benzothiophene-3-ylmethylsulfamide
FMRF-amide	Phe-Met-Arg-Phe-NH2 peptide
GABA	γ - Aminobutyric acid
GAD	glutamic acid decarboxylase
GMP	Guanosine monophosphate
HEPES	2-[4-(2-hydroxyethyl)piperazin-1-yl]ethanesulfonic acid
HC	Horizontal Cell
I_{Ca}	Ca^{2+} current
i.d.	Inner diameter
$I_{feedback}$	Feedback current
iGluR	Ionotropic glutamate receptor
I_{inward}	Inward current
I_m	Membrane current
INL	Inner nuclear layer

IPL	Inner plexiform layer
ipRGC	Intrinsically photosensitive retinal ganglion cell
I - V plot	Current versus voltage plot
$I_{outward}$	Outward current
I_{peak}	Peak current
IS	Inner segment
NA	Numerical aperture
NBC	Sodium-bicarbonate cotransporter
NHE	Na^+/H^+ exchanger
NT	Neurotransmitter
o.d.	Outer diameter
ONL	Outer nuclear layer
OPL	Outer plexiform layer
OS	Outer segment
PDE	phosphodiesterase
PR	Photoreceptor
RGC	Retinal ganglion cell
V_{50}	voltage when I_{peak} is half-maximal;
V-ATPase	vacuolar-type H^+- ATPase
VGCC	Voltage-gated Ca^{2+} channel
V_m	Membrane potential
zoniporide	N-(diaminomethylidene)-3-methanesulfonyl-4-(propan-2-yl)benzamide

Appendix B: References

Anthologies

Kawamura S & S Tachibanaki. 2014. Phototransduction in Rods and Cones. *Vertebrate Photoreceptors: Functional Molecular Bases*. Furukawa, Y, JB Hurley, & S Kawamura, editors. Springer, Tokyo. 167-198.

Pierantoni RL, McCann GD. A quantitative study on synaptic ribbons in the photoreceptors of turtle and frog. In: Borsellino A, Cervetto L, editors. *Photoreceptors*. New York: Plenum Press; 1981. pp. 255–283.

Books

Byrne JH, Roberts JL. *From Molecules to Networks: An Introduction to Cellular and Molecular Neuroscience, 2nd Ed*. Academic Press, Elsevier Inc., 2009, 2004.

Dowling JE. *The Retina: An Approachable Part of the Brain*. The Belknap Press of Harvard University Press. 2012.

Hille B. *Ionic Channels of Excitable Membranes*, 2nd Ed. Sinauer Associates Inc. 1992.

Kandel ER, JH Schwartz, & TM Jessell. *Principles of Neuroscience, 4th Ed*. The McGraw-Hill Companies Inc., 2000.

Ogden D (ed.). *Microelectrode Techniques: The Plymouth Workshop Handbook*, 2nd Ed. The Company of Biologists Limited, 1987.

Rodieck RW. *The First Steps in Seeing*. Sinauer Associates, Inc. 1988.

Sarthy V, Ripps H. *The Retinal Müller Cell: Structure and Function*. Springer Science & Business Media, 2001.

Journal references

Ahnelt PK, Keri C, Kolb H. Identification of pedicles of putative blue sensitive cones in human and primate retina. *Journal of Comparative Neurology*. 1990;293:39–53.

Babai N, Thoreson WB. Horizontal cell feedback regulates calcium currents and intracellular calcium levels in rod photoreceptors of salamander and mouse retina. *Journal of Physiology*. 2009 May 15;587(Pt 10):2353-64.

Ball SL, Powers PA, Shin HS, Morgans CW, Peachey NS, Gregg RG. Role of the beta(2) subunit of voltage-dependent calcium channels in the retinal outer plexiform layer. *Investigative Ophthalmology and Visual Sciences*. 2002 May;43(5):1595-603.

Barnes, S., V. Merchant, and F. Mahmud. 1993. Modulation of transmission gain by protons at the photoreceptor output synapse. *Proceedings of the National Academy of the Sciences of the United States of America*. 90:10081–10085.

Bartoletti TM, Babai N, Thoreson WB. Vesicle pool size at the salamander cone ribbon synapse. *Journal of Neurophysiology*. 2010 Jan;103(1):419-23.

Baumann L, Gerstner A, Zong X, Biel M, Wahl-Schott C. Functional characterization of the L-type Ca2+-channel Cav1.4α1 from mouse retina. *Investigative Ophthalmology and Visual Science*., 45 (2004), pp. 708–713.

Baylor DA, Fettiplace R. Transmission from photoreceptors to ganglion cells in turtle retina. *Journal of Physiology*. 1977 Oct;271(2):391-424.

Baylor DA, Fuortes MG, O'Bryan PM. 1971. Receptive fields of cones in the retina of the turtle. *The Journal of Physiology*. 1971 Apr;214(2):265-94.

Baylor DA, Nunn BJ, Schnapf JL. Spectral sensitivity of cones of the monkey Macaca fascicularis. *Journal of Physiology*. 1987 Sep;390:145-60.

Bech-Hansen NT, Naylor MJ, Maybaum TA, Pearce WG, Koop B, Fishman GA, Mets M, Musarella MA, Boycott KM. Loss-of-function mutations in a calcium-channel alpha1-subunit gene in Xp11.23 cause incomplete X-linked congenital stationary night blindness. *Nature Genetics*. 1998 Jul;19(3):264-7.

Bloomfield SA, Dowling JE. Roles of aspartate and glutamate in synaptic transmission in rabbit retina. I. Outer plexiform layer. *Journal of Neurophysiology*. 1985 Mar;53(3):699-713.

Blot A, Barbour B. Ultra-rapid axon-axon ephaptic inhibition of cerebellar Purkinje cells by the pinceau. *Nature Neuroscience*. 2014 Feb;17(2):289-95.

Borghuis BG, Looger LL, Tomita S, Demb JB. Kainate receptors mediate signaling in both transient and sustained OFF bipolar cell pathways in mouse retina. *The Journal of Neuroscience*. 2014 Apr 30;34(18):6128-39.

Burkhardt DA, Gottesman J, Thoreson WB. Prolonged depolarization in turtle cones evoked by current injection and stimulation of the receptive field surround. *The Journal of Physiology*. 1988 Dec;407:329-48.

Byzov AL. Origin of non-linearity of voltage--current relationships of turtle cones. *Vision Res*earch. 1979;19(5):469-77.

Byzov AL, Shura-Bura TM. Electrical feedback mechanism in the processing of signals in the outer plexiform layer of the retina. *Vision Research*. 1986;26(1):33-44.

Cadetti L, Thoreson WB. Feedback effects of horizontal cell membrane potential on cone calcium currents studied with simultaneous recordings. *Journal of*

Neurophysiology. 2006 Mar;95(3):1992-5.

Carbone AL, Plested AJ. Coupled control of desensitization and gating by the ligand binding domain of glutamate receptors. *Neuron*. 2012 Jun 7;74(5):845-57.

Chen M, Križaj D, Thoreson WB. Intracellular calcium stores drive slow non-ribbon vesicle release from rod photoreceptors. *Frontiers in Cellular Neuroscience*. 2014 Feb 3;8:20.

Chen M, Van Hook MJ, Zenisek D, Thoreson WB. Properties of ribbon and non-ribbon release from rod photoreceptors revealed by visualizing individual synaptic vesicles. *The Journal of neuroscience: the official journal of the society of neuroscience*. 2013 Jan 30;33(5):2071-86.

Chen RS, Deng TC, Garcia T, Sellers ZM, Best PM. Calcium channel gamma subunits: a functionally diverse protein family. *Cell Biochemistry and Biophysics*. 2007;47(2):178-86.

Chen XH, Tsien RW. Aspartate substitutions establish the concerted action of P-region glutamates in repeats I and III in forming the protonation site of L-type Ca2+ channels. *The Journal of Biological Chemistry*. 1997 Nov 28;272(48):30002-8.

Corey DP, Dubinsky JM, Schwartz EA. The calcium current in inner segments of rods from the salamander (Ambystoma tigrinum) retina. *The Journal of Physiology*. 1984 Sep;354:557-75.

Crook JD, Davenport CM, Peterson BB, Packer OS, Detwiler PB, Dacey DM. Parallel ON and OFF cone bipolar inputs establish spatially coextensive receptive field structure of blue-yellow ganglion cells in primate retina. *The Journal of Neuroscience*. 2009 Jul 1;29(26):8372-87.

Crook JD, Manookin MB, Packer OS, Dacey DM. Horizontal cell feedback without cone type-selective inhibition mediates "red-green" color opponency in midget ganglion cells of the primate retina. *The Journal of Neuroscience*. 2011 Feb 2;31(5):1762-72.

Dacey DM, Lee BB, Stafford DK, Pokorny J, Smith VC. Horizontal cells of the primate retina: cone specificity without spectral opponency. *Science*, 271 (1996), pp. 656–659.

Deeb SS, Diller LC, Williams DR, Dacey DM. Interindividual and topographical variation of L:M cone ratios in monkey retinas. *Journal of the Optical Society of America. A, Optics, Image Science, and Vision*. 2000;17(3):538–44.

Demaurex N, Orlowski J, Brisseau G, Woodside M, Grinstein S. The mammalian Na+/H+ antiporters NHE-1, NHE-2, and NHE-3 are electroneutral and voltage independent, but can couple to an H+ conductance. *The Journal of General Physiology*. 1995 Jul;106(1):85-111.

DeVries SH.Exocytosed protons feedback to suppress the Ca^{2+} current in mammalian cone photoreceptors. *Neuron*. 2001 Dec 20;32(6):1107-17.

DeVries SH, Li W, Saszik S. Parallel processing in two transmitter microenvironments at the cone photoreceptor synapse. *Neuron*. 2006 Jun 1;50(5):735-48.

Dhingra A, Lyubarsky A, Jiang M, Pugh EN Jr, Birnbaumer L, Sterling P, Vardi N. The light response of ON bipolar neurons requires G[alpha]o. *The Journal of Neuroscience*. 2000 Dec 15;20(24):9053-8.

Dmitriev AV, Mangel SC. Electrical feedback in the cone pedicle: a computational analysis. *Journal of Neurophysiology*. 2006 Mar;95(3):1419-27.

Doering CJ, Hamid J, Simms B, McRory JE, Zamponi GW. Cav1.4 encodes a calcium channel with low open probability and unitary conductance. *Biophysical Journal*. 2005 Nov;89(5):3042-8.

Doering CJ, McRory JE. Effects of extracellular pH on neuronal calcium channel activation. *Neuroscience*. 2007 May 25;146(3):1032-43. Epub 2007 Apr 16

Dolphin AC. Calcium channel auxiliary α2δ and β subunits: trafficking and one step beyond. *Nature Reviews Neuroscience*. 2012 Jul 18;13(8):542-55.

Endeman D, Fahrenfort I, Sjoerdsma T, Steijaert M, Ten Eikelder H, Kamermans M. Chloride currents in cones modify feedback from horizontal cells to cones in goldfish retina. *Journal of Physiology*. 2012 Nov 15;590(Pt 22):5581-95.

Fahrenfort I, Steijaert M, Sjoerdsma T, Vickers E, Ripps H, van Asselt J, Endeman D, Klooster J, Numan R, ten Eikelder H, von Gersdorff H, Kamermans M. Hemichannel-mediated and pH-based feedback from horizontal cells to cones in the vertebrate retina. *PLoS One*. 2009;4:e6090.

Feigenspan A, Babai N. Functional properties of spontaneous excitatory currents and encoding of light/dark transitions in horizontal cells of the mouse retina. *The European Journal of Neuroscience*. 2015 Nov;42(9):2615-32.

Fiaschi T, Giannoni E, Taddei ML, Cirri P, Marini A, Pintus G, Nativi C, Richichi B, Scozzafava A, Carta F, Torre E, Supuran CT, Chiarugi P. Carbonic anhydrase IX from cancer-associated fibroblasts drives epithelial-mesenchymal transition in prostate carcinoma cells. *Cell Cycle*. 2013 Jun 1;12(11):1791-801.

Fuortes MG, Schwartz EA, Simon EJ. Colour-dependence of cone responses in the turtle retina. *The Journal of Physiology*. 1973 Oct;234(1):199-216.

Fuster D, Moe OW, Hilgemann DW. Lipid- and mechanosensitivities of sodium/hydrogen exchangers analyzed by electrical methods. *Proceedings of the National Academy of the Sciences in the United States of America*. 2004 Jul 13;101(28):10482-7.

Gardner CL, Jones JR, Baer SM, Crook SM. Drift-diffusion simulation of the ephaptic effect in the triad synapse of the retina. *Journal of Computational Neuroscience*. 2015 Feb;38(1):129-42.

Gerschenfeld HM, Piccolino M. Different effects of applied currents during central and peripheral illumination of *Pseudemys* turtle cones [proceedings]. *Journal of Physiology*. 1978 Jul;280:49P-50P.

Gerschenfeld HM, Piccolino M, Neyton J. Feed-back modulation of cone synapses by L-horizontal cells of turtle retina. *Journal of Experimental Biology*. 1980 Dec;89:177-92.

Guo C, Stella SL Jr, Hirano AA, Brecha NC. Plasmalemmal and vesicular gamma-aminobutyric acid transporter expression in the developing mouse retina. The *Journal of Comparative Neurology*. 2009 Jan 1;512(1):6-26.

Halligan RD, Shelat H, Kahn AM. Na(+)-independent Cl(-)-HCO3- exchange in sarcolemmal vesicles from vascular smooth muscle. *The American Journal of Physiology*. 1991 Feb;260(2 Pt 1):C347-54.

Hare WA, Owen WG. Receptive field of the retinal bipolar cell: a pharmacological study in the tiger salamander. *The Journal of Neurophysiology*. 1996 Sep;76(3):2005-19.

Hartline HK, Wagner HG, Ratliff F. Inhibition in the eye of Limulus. Journal of General Physiology. 1956 May 20;39(5):651-73.

Haugh-Scheidt L, Ripps H. pH regulation in horizontal cells of the skate retina. *Experimental Eye Research*. 1998 Apr;66(4):449-63.

Haverkamp S, Grünert U, Wässle H. Localization of kainate receptors at the cone pedicles of the primate retina. *Journal of Comparative Neurology*, 436 (2001a), pp. 471–486.

Haverkamp S, Grünert U, Wässle H. The synaptic architecture of AMPA receptors at the cone pedicle of the primate retina. *Journal of Comparative Neurology*, 436 (2001b), pp. 471–486.

Hecht S, Shlaer S, Pirenne MH. ENERGY, QUANTA, AND VISION. *The Journal of General Physiology*. 1942 Jul 20;25(6):819-40.

Hess P, Lansman JB, Tsien RW. Calcium channel selectivity for divalent and monovalent cations. Voltage and concentration dependence of single channel current in ventricular heart cells. *Journal of General Physiology*. 1986 Sep;88(3):293-319.

Hirano AA, Brandstätter JH, Morgans CW, Brecha NC. SNAP25 expression in mammalian retinal horizontal cells. *The Journal of Comparative Neurology*. 2011

Apr 1;519(5):972-88.

Hirano AA, Brandstätter JH, Vila A, Brecha NC. Robust syntaxin-4 immunoreactivity in mammalian horizontal cell processes. *Visual Neuroscience*. 2007 Jul-Aug;24(4):489-502.

Hirasawa H, Kaneko A. pH changes in the invaginating synaptic cleft mediate feedback from horizontal cells to cone photoreceptors by modulating Ca2+ channels. *The Journal of General Physiology*. 2003 Dec;122(6):657-71.

Jackman SL, Babai N, Chambers JJ, Thoreson WB, Kramer RH. A positive feedback synapse from retinal horizontal cells to cone photoreceptors. *PLoS Biology*. 2011 May;9(5):e1001057.

Jackman SL, Choi SY, Thoreson WB, Rabl K, Bartoletti TM, Kramer RH. Role of the synaptic ribbon in transmitting the cone light response. *Nature Neuroscience*. 2009 Mar;12(3):303-10.Jacoby J, Kreitzer MA, Alford S, Qian H, Tchernookova BK, Naylor ER, Malchow RP. Extracellular pH dynamics of retinal horizontal cells examined using electrochemical and fluorometric methods. *Journal of Neurophysiology*. 2012;107:868–79.

Janssen-Bienhold U, Schultz K, Hoppenstedt W, Weiler R. Molecular diversity of gap junctions between horizontal cells. *Progress in Brain Research*. 2001;131:93-107.

Jouhou H, Yamamoto K, Homma A, Hara M, Kaneko A, Yamada M. Depolarization of isolated horizontal cells of fish acidifies their immediate surrounding by activating V-ATPase. *The Journal of Physiology*. 2007 Dec 1;585(Pt 2):401-12. Epub 2007 Oct 11.

Kamermans M, Fahrenfort I, Schultz K, Janssen-Bienhold U, Sjoerdsma T, Weiler R. Hemichannel-mediated inhibition in the outer retina. *Science*. 2001 May 11;292(5519):1178-80.

Kamiji NL, Yamamoto K, Hirasawa H, Yamada M, Usui S, Kurokawa M. Proton feedback mediates the cascade of color-opponent signals onto H3 horizontal cells in goldfish retina. *Neuroscience Research*. 2012 Apr;72(4):306-15.

Kaneko A. Electrical connexions between horizontal cells in the dogfish retina. *Journal of Physiology*. 1971 Feb;213(1):95-105.

Kao L, Kurtz LM, Shao X, Papadopoulos MC, Liu L, Bok D, Nusinowitz S, Chen B, Stella SL, Andre M, Weinreb J, Luong SS, Piri N, Kwong JM, Newman D, Kurtz I. Severe neurologic impairment in mice with targeted disruption of the electrogenic sodium bicarbonate cotransporter NBCe2 (Slc4a5 gene). *The Journal of Biological Chemistry*. 2011 Sep 16;286(37):32563-74.

Kemmler R, Schultz K, Dedek K, Euler T, Schubert T. Differential regulation of cone

calcium signals by different horizontal cell feedback mechanisms in the mouse retina. *Journal of Neuroscience*. 2014 Aug 27;34(35):11826-43.

Klaassen LJ, Sun Z, Steijaert MN, Bolte P, Fahrenfort I, Sjoerdsma T, Klooster J, Claassen Y, Shields CR, Ten Eikelder HM, Janssen-Bienhold U, Zoidl G, McMahon DG, Kamermans M. Synaptic transmission from horizontal cells to cones is impaired by loss of connexin hemichannels. *PLoS Biology*. 2011 Jul;9(7):e1001107.

Kobayashi S, Morgans CW, Casey JR, Kopito RR. AE3 anion exchanger isoforms in the vertebrate retina: developmental regulation and differential expression in neurons and glia. *The Journal of Neuroscience*. 1994 Oct;14(10):6266-79.

Koike C, Obara T, Uriu Y, Numata T, Sanuki R, Miyata K, Koyasu T, Ueno S, Funabiki K, Tani A, Ueda H, Kondo M, Mori Y, Tachibana M, Furukawa T. TRPM1 is a component of the retinal ON bipolar cell transduction channel in the mGluR6 cascade. *Proceedings of the National Academy of the Sciences in the United States of America*. 2010 Jan 5;107(1):332-7.

Koschak A, Reimer D, Walter D, Hoda JC, Heinzle T, Grabner M, Striessnig J. Cav1.4alpha1 subunits can form slowly inactivating dihydropyridine-sensitive L-type Ca2+ channels lacking Ca2+-dependent inactivation. *The Journal of Neuroscience*. 2003 Jul 9;23(14):6041-9.

Koskelainen A, Donner K, Lerber T, Hemilä S. pH regulation in frog cones studied by mass receptor photoresponses from the isolated retina. *Vision Research*. 1993 Nov;33(16):2181-8.

Krafte DS, Kass RS. Hydrogen ion modulation of Ca channel current in cardiac ventricular cells. Evidence for multiple mechanisms. *The Journal of General Physiology*. 1988 May;91(5):641-57.

Kuffler SW. Discharge patterns and functional organization of mammalian retina. *Journal of Neurophysiology*. 1953 Jan;16(1):37-68.

Lam DM. Biosynthesis of gamma-aminobutyric acid by isolated axons of cone horizontal cells in the goldfish retina. *Nature*. 1975 Mar 27;254(5498):345-7.

Lam DM, Steinman L. The uptake of (- 3 H) aminobutyric acid in the goldfish retina. *Proceedings of the National Academy of the Sciences of the United States of America*. 1971 Nov;68(11):2777-81.

Lasansky A. Organization of the outer synaptic layer in the retina of the larval tiger salamander. *Philosophical Transactions of the Royal Society of London. Series B, Biological Sciences*. 1973;265(872):471-89.

Lasater EM, Dowling JE. Dopamine decreases conductance of the electrical junctions between cultured retinal horizontal cells. *Proceedings of the National Academy of*

the Sciences of the United States of America. 1985 May;82(9):3025-9.

Lee A, Wang S, Williams B, Hagen J, Scheetz TE, Haeseleer F. Characterization of Cav1.4 complexes (α11.4, β2, and α2δ4) in HEK293T cells and in the retina. *Journal of Biological Chemistry*. 2015 Jan 16;290(3):1505-21.

Lee H, Brecha NC. Immunocytochemical evidence for SNARE protein-dependent transmitter release from guinea pig horizontal cells. *The European Journal of Neuroscience*. 2010 Apr;31(8):1388-401.

Lee S, Chen L, Chen M, Ye M, Seal RP, Zhou ZJ. An unconventional glutamatergic circuit in the retina formed by vGluT3 amacrine cells. *Neuron*. 2014 Nov 19;84(4):708-15.

Lindstrom SH, Ryan DG, Shi J, DeVries SH. Kainate receptor subunit diversity underlying response diversity in retinal off bipolar cells. *The Journal of Physiology*. 2014 Apr 1;592(Pt 7):1457-77.

Liu X, Hirano AA, Sun X, Brecha NC, Barnes S. Calcium channels in rat horizontal cells regulate feedback inhibition of photoreceptors through an unconventional GABA- and pH-sensitive mechanism. *Journal of Physiology*. 2013 Jul;591(13):3309-24.

Liu Y, Edwards RH (1997) The role of vesicular transport proteins in synaptic transmission and neural degeneration. *Annual Review of Neuroscience*. 20: 125-156.

LoGiudice L, Matthews G. The role of ribbons at sensory synapses. *Neuroscientist*. 2009 Aug;15(4):380-91.

Mangel SC. Analysis of the horizontal cell contribution to the receptive field surround of ganglion cells in the rabbit retina. *Journal of Physiology*. 1991 Oct;442:211-34

McMahon MJ, Packer OS, Dacey DM. The classical receptive field surround of primate parasol ganglion cells is mediated primarily by a non-GABAergic pathway. *Journal of Neuroscience*. 2004 Apr 14;24(15):3736-45.

Migdale K, Herr S, Klug K, Ahmad K, Linberg K, Sterling P, Schein S. Two ribbon synaptic units in rod photoreceptors of macaque, human, and cat. *The Journal of Comparative Neurology*. 2003 Jan 1;455(1):100-12.

Morgans CW. Localization of the alpha(1F) calcium channel subunit in the rat retina. *Investigative Ophthalmololgy & Visual Science*. 2001 Sep; 42(10):2414-8.

Morgans CW, Zhang J, Jeffrey BG, Nelson SM, Burke NS, Duvoisin RM, Brown RL. TRPM1 is required for the depolarizing light response in retinal ON-bipolar cells. *The Proceedings of the National Academy of the Sciences in the United States of America*. 2009 Nov 10;106(45):19174-8.

Nachman-Clewner M, St Jules R, Townes-Anderson E. L-type calcium channels in the photoreceptor ribbon synapse: localization and role in plasticity. *Journal of Comparative Neurology*. 1999 Dec 6;415(1):1-16.

Nagelhus EA, Mathiisen TM, Bateman AC, Haug FM, Ottersen OP, Grubb JH, Waheed A, Sly WS. Carbonic anhydrase XIV is enriched in specific membrane domains of retinal pigment epithelium, Muller cells, and astrocytes. *Proceedings of the National Academy of the Sciences in the United States of America*. 2005 May 31;102(22):8030-5.

Naka KI, Rushton WA. The generation and spread of S-potentials in fish (Cyprinidae). *Journal of Physiol*ogy. 1967 Sep;192(2):437-61.

Negishi K, Salas R, Laufer M. Origins of horizontal cell spectral responses in the retina of marine teleosts (Centropomus and Mugil sp). *Journal of Neuroscience Research*. 1997 Jan 1;47(1):68-76.

Nelson R, von Litzow A, Kolb H, Gouras P. Horizontal cells in cat retina with independent dendritic systems. *Science*. 1975 Jul 11;189(4197):137-9.

O'Bryan PM. Properties of the depolarizing synaptic potential evoked by peripheral illumination in cones of the turtle retina. *The Journal of Physiology*. 1973 Nov;235(1):207-23.

Ohmori H, Yoshii M. Surface potential reflected in both gating and permeation mechanisms of sodium and calcium channels of the tunicate egg cell membrane. *Journal of Physiology*. 1977 May;267(2):429-63.

Otis T, Zhang S, Trussell LO. Direct measurement of AMPA receptor desensitization induced by glutamatergic synaptic transmission. *The Journal of Neuroscience*. 1996 Dec 1;16(23):7496-504.

Packer OS, Verweij J, Li PH, Schnapf JL, Dacey DM. Blue-yellow opponency in primate S cone photoreceptors. *Journal of Neuroscience*. 2010 Jan 13;30(2):568-72.

Pan F, Massey SC. Rod and cone input to horizontal cells in the rabbit retina. *Journal of Comparative Neurology*. 2007 Feb 10;500(5):815-31.

Pang JJ, Gao F, Barrow A, Jacoby RA, Wu SM. How do tonic glutamatergic synapses evade receptor desensitization? *Journal of Physiology*. 2008 Jun 15;586(Pt 12):2889-902.

Perlman I, Knapp AG, Dowling JE. Responses of isolated white perch horizontal cells to changes in the concentration of photoreceptor transmitter agonists. *Brain Research*. 1989 May 15;487(1):16-25.

Petrov AM, Naumenko NV, Uzinskaya KV, Giniatullin AR, Urazaev AK, Zefirov AL. Increased non-quantal release of acetylcholine after inhibition of endocytosis by

methyl-β-cyclodextrin: the role of vesicular acetylcholine transporter. *Neuroscience*. 2011 Jul 14;186:1-12

Piccolino M, Gerschenfeld HM. Activation of a regenerative calcium conductance in turtle cones by peripheral stimulation. *Proceedings of the Royal Society of London, Series B Biological Sciences*. 1978 May 16;201(1144):309-15.

Prod'hom B, Pietrobon D, Hess P. Direct measurement of proton transfer rates to a group controlling the dihydropyridine-sensitive Ca2+ channel. *Nature*, 329 (1987), pp. 243–246.

Puller C, Ivanova E, Euler T, Haverkamp S, Schubert T. OFF bipolar cells express distinct types of dendritic glutamate receptors in the mouse retina. *Neuroscience*. 2013 Jul 23;243:136-48.

Puthussery T, Percival KA, Venkataramani S, Gayet-Primo J, Grünert U, Taylor WR. Kainate receptors mediate synaptic input to transient and sustained OFF visual pathways in primate retina. *The Journal of Neuroscience*. 2014 May 28;34(22):7611-21.

Rao-Mirotznik R, Harkins AB, Buchsbaum G, Sterling P. Mammalian rod terminal: architecture of a binary synapse. *Neuron*. 1995 Mar;14(3):561-9.

Ratliff F, Hartline HK. The responses of Limulus optic nerve fibers to patterns of illumination on the receptor mosaic. *Journal of General Physiology*. 1959 Jul 20;42(6):1241-55.

Raviola E, Gilula NB. Gap junctions between photoreceptor cells in the vertebrate retina. *Proceedings of the National Academy of the Sciences in the United States of America*. 1973 Jun;70(6):1677-81.

Ribelayga C, Wang Y, Mangel SC. Dopamine mediates circadian clock regulation of rod and cone input to fish retinal horizontal cells. *Journal of Physiology*. 2002 Nov 1;544(Pt 3):801-16.

Romero MF, Chen AP, Parker MD, Boron WF. The SLC4 family of bicarbonate (HCO_3^-) transporters. *Molecular Aspects of Medicine*. 2013 Apr-Jun;34(2-3):159-82.

Romero MF, Hediger MA, Boulpaep EL, Boron WF. Expression cloning and characterization of a renal electrogenic Na+/HCO3- cotransporter. *Nature*. 1997 May 22;387(6631):409-13.

Schmidt TM, Alam NM, Chen S, Kofuji P, Li W, Prusky GT, Hattar S. A role for melanopsin in alpha retinal ganglion cells and contrast detection. *Neuron*. 2014 May 21;82(4):781-8.

Schwartz EA. Calcium-independent release of GABA from isolated horizontal cells of the toad retina. *Journal of Physiology*. 1982 Feb;323:211-27.

Shelley J, Dedek K, Schubert T, Feigenspan A, Schultz K, Hombach S, Willecke K, Weiler R. Horizontal cell receptive fields are reduced in connexin57-deficient mice. *European Journal of Neuroscience*. 2006 Jun;23(12):3176-86.

Shen Y, Heimel JA, Kamermans M, Peachey NS, Gregg RG, Nawy S. A transient receptor potential-like channel mediates synaptic transmission in rod bipolar cells. *The Journal of Neuroscience*. 2009 May 13;29(19):6088-93.

Shen Y, Rampino MA, Carroll RC, Nawy S. G-protein-mediated inhibition of the Trp channel TRPM1 requires the Gβγ dimer. *Proceedings of the Nationall Academy of the Sciences in the United States of America*. 2012 May 29;109(22):8752-7.

Sherry DM, Bui DD, Degrip WJ. Identification and distribution of photoreceptor subtypes in the neotenic tiger salamander retina. *Visual Neuroscience*. 1998 Nov-Dec;15(6):1175-87.

Shiells RA, Falk G, Naghshineh S. Action of glutamate and aspartate analogues on rod horizontal and bipolar cells. *Nature*. 1981 Dec 10; 294(5841):592-4.

Shmukler BE, Reimold FR, Heneghan JF, Chen C, Zhao T, Paw BH, Alper SL. Molecular cloning and functional characterization of zebrafish Slc4a3/Ae3 anion exchanger. *Pflügers Archiv: European Journal of Physiology*. 2014 Aug;466(8):1605-18.

Siegert S, Cabuy E, Scherf BG, Kohler H, Panda S, Le YZ, Fehling HJ, Gaidatzis D, Stadler MB, Roska B. Transcriptional code and disease map for adult retinal cell types. *Nature Neuroscience*. 2012 Jan 22;15(3):487-95, S1-2.

Snellman J, Kaur T, Shen Y, Nawy S. Regulation of ON bipolar cell activity. *Progress in Retinal Eye Research*. 2008 Jul;27(4):450-63.

Snellman J, Mehta B, Babai N, Bartoletti TM, Akmentin W, Francis A, Matthews G, Thoreson W, Zenisek D. Acute destruction of the synaptic ribbon reveals a role for the ribbon in vesicle priming. *Nature Neuroscience*. 2011 Jul 24;14(9):1135-41.

Stell WK, Lightfoot DO. Color-specific interconnections of cones and horizontal cells in the retina of the goldfish. *Journal of Comparative Neurology*. 1975 Feb 15;159(4):473-502.

Sterling P, Matthews G. Structure and function of ribbon synapses. *Trends in Neuroscience*. 2005 Jan;28(1):20-9.

Strom TM, Nyakatura G, Apfelstedt-Sylla E, Hellebrand H, Lorenz B, Weber BH, Wutz K, Gutwillinger N, Rüther K, Drescher B, Sauer C, Zrenner E, Meitinger T, Rosenthal A, Meindl A. An L-type calcium-channel gene mutated in incomplete X-linked congenital stationary night blindness. *Nature Genetics*. 1998 Jul;19(3):260-3.

Su CY, Menuz K, Reisert J, Carlson JR. Non-synaptic inhibition between grouped neurons in an olfactory circuit. *Nature*. 2012 Dec 6;492(7427):66-71.

Supuran CT, Scozzafava A. Benzolamide is not a membrane-impermeant carbonic anhydrase inhibitor. *Journal of Enzyme Inhibition and Medicinal Chemistry*. 2004 Jun;19(3):269-73.

Tachibana M, Kaneko A. Gamma-aminobutyric acid acts at axon terminals of turtle photoreceptors: difference in sensitivity among cell types. *Proceedings of the National Academy of the Sciences of the United States of America*, 81 (1984), pp. 7961–7964.

Tang L, Gamal El-Din TM, Payandeh J, Martinez GQ, Heard TM, Scheuer T, Zheng N, Catterall WA. Structural basis for Ca^{2+} selectivity of a voltage-gated calcium channel. *Nature*. 2014 Jan 2;505(7481):56-61.

Tatsukawa T, Hirasawa H, Kaneko A, Kaneda M. GABA-mediated component in the feedback response of turtle retinal cones. *Visual Neuroscience*. 2005 May-Jun;22(3):317-24.

Thoreson WB, Babai N, Bartoletti TM. Feedback from horizontal cells to rod photoreceptors in vertebrate retina. *Journal of Neuroscience*. 2008 May 28;28(22):5691-5.

Thoreson WB, Bryson EJ. Chloride equilibrium potential in salamander cones. *BMC Neuroscience*. 2004 Dec 5;5:53.

Thoreson WB, Burkhardt DA. Effects of synaptic blocking agents on the depolarizing responses of turtle cones evoked by surround illumination. *Visual Neuroscience*. 1990 Dec;5(6):571-83.

Thoreson WB, Rabl K, Townes-Anderson E, Heidelberger R. A highly Ca2+-sensitive pool of vesicles contributes to linearity at the rod photoreceptor ribbon synapse. *Neuron*. 2004 May 27;42(4):595-605.

Tomita T. Electrophysiological study of the mechanisms subserving color coding in the fish retina. *Cold Spring Harbor Symposia on Quantitative Biology*. 1965;30:559-66.

tom Dieck S, Altrock WD, Kessels MM, Qualmann B, Regus H, Brauner D, Fejtová A, Bracko O, Gundelfinger ED, Brandstätter JH. Molecular dissection of the photoreceptor ribbon synapse: physical interaction of Bassoon and RIBEYE is essential for the assembly of the ribbon complex. *Journal of Cell Biology*. 2005 Feb 28; 168(5):825-36.

Toyoda J, Nosaki H, Tomita T. Light-induced resistance changes in single photoreceptors of Necturus and Gekko. *Vision Research*. 1969 Apr;9(4):453-63.

Trenholm S, Baldridge WH. The effect of aminosulfonate buffers on the light responses and intracellular pH of goldfish retinal horizontal cells. *Journal of Neurochemistry*. 2010;115:102–11.

Trümpler J, Dedek K, Schubert T, de Sevilla Müller LP, Seeliger M, Humphries P, Biel M, Weiler R. Rod and cone contributions to horizontal cell light responses in the mouse retina. *The Journal of Neuroscience*. 2008 Jul 2;28(27):6818-25.

van der Velden. The number of quanta necessary for the perception of light of the human eye. *Ophthalmologica*. 1946 Jun;111(6):321-31.

Van Hook MJ, Thoreson WB. Simultaneous whole-cell recordings from photoreceptors and second-order neurons in an amphibian retinal slice preparation. Journal of Visualized Experiments: JoVE. 2013 Jun 1;(76).

Verweij J, Dacey DM, Peterson BB, Buck SL. Sensitivity and dynamics of rod signals in H1 horizontal cells of the macaque monkey retina. *Vision Research*. 1999 Nov;39(22):3662-72.

Verweij J, Hornstein EP, Schnapf JL. Surround antagonism in macaque cone photoreceptors. *The Journal of Neuroscience*. 2003 Nov 12;23(32):10249-57.

Verweij J, Kamermans M, Spekreijse H. Horizontal cells feed back to cones by shifting the cone calcium-current activation range. *Vision Research*. 1996 Dec;36(24):3943-53.

Vessey JP, Lalonde MR, Mizan HA, Welch NC, Kelly ME, Barnes S. Carbenoxolone inhibition of voltage-gated Ca channels and synaptic transmission in the retina. *Journal of Neurophysiology*. 2004 Aug;92(2):1252-6.

Vessey JP, Stratis AK, Daniels BA, Da Silva N, Jonz MG, Lalonde MR, Baldridge WH, Barnes S. Proton-mediated feedback inhibition of presynaptic calcium channels at the cone photoreceptor synapse. *Journal of Neuroscience*. 2005 Apr 20;25(16):4108-17.

Vigh J, Witkovsky P. Sub-millimolar cobalt selectively inhibits the receptive field surround of retinal neurons. *Visual Neuroscience*. 1999 Jan-Feb;16(1):159-68.

Virkki LV, Wilson DA, Vaughan-Jones RD, Boron WF. Functional characterization of human NBC4 as an electrogenic Na+-HCO cotransporter (NBCe2). *American Journal of Physiology. Cell Physiology*. 2002 Jun;282(6):C1278-89.

Vroman R, Klaassen LJ, Howlett MH, Cenedese V, Klooster J, Sjoerdsma T, Kamermans M. Extracellular ATP hydrolysis inhibits synaptic transmission by increasing ph buffering in the synaptic cleft. *PLoS Biology*. 2014 May 20;12(5):e1001864.

Wahl-Schott C, Baumann L, Cuny H, Eckert C, Griessmeier K, Biel M. Switching off calcium-dependent inactivation in L-type calcium channels by an autoinhibitory

domain. *Proceedings of the National Academy of the Sciences in the United States of America*. 2006 Oct 17;103(42):15657-62.

Wang TM, Holzhausen LC, Kramer RH. Imaging an optogenetic pH sensor reveals that protons mediate lateral inhibition in the retina. *Nature Neuroscience*. 2014 Feb;17(2):262-8.

Weckström M, Laughlin S. Also blowfish eye has a very good example Extracellular potentials modify the transfer of information at photoreceptor output synapses in the blowfly compound eye. *The Journal of Neuroscience*. 2010 Jul 14;30(28):9557-66.

Wiesel TN, Hubel DH. Spatial and chromatic interactions in the lateral geniculate body of the rhesus monkey. *Journal of Neurophysiology*. 1966 Nov;29(6):1115-56.

Wilkinson MF, Barnes S. The dihydropyridine-sensitive calcium channel subtype in cone photoreceptors. *Journal of General Physiology*. 1996 May;107(5):621-30.

Winum JY, Thiry A, Cheikh KE, Dogné JM, Montero JL, Vullo D, Scozzafava A, Masereel B, Supuran CT. Carbonic anhydrase inhibitors. Inhibition of isoforms I, II, IV, VA, VII, IX, and XIV with sulfonamides incorporating fructopyranose-thioureido tails. *Bioorganic and Medicinal Chemistry Letters.* 2007 May 15;17(10):2685-91.

Wu SM. Input-output relations of the feedback synapse between horizontal cells and cones in the tiger salamander retina. *Journal of Neurophysiology*. 1991 May;65(5):1197-206.

Wycisk KA, Zeitz C, Feil S, Wittmer M, Forster U, Neidhardt J, Wissinger B, Zrenner E, Wilke R, Kohl S, Berger W. Mutation in the auxiliary calcium-channel subunit CACNA2D4 causes autosomal recessive cone dystrophy. *American Journal of Human Genetics*. 2006 Nov;79(5):973-7.

Yang D, Gereau RW 4th. Group II metabotropic glutamate receptors inhibit cAMP-dependent protein kinase-mediated enhancemednt of tetrodotoxin-resistant sodium currents in mouse dorsal root ganglion neurons. *Neuroscience Letters*. 2004 Mar 11;357(3):159-62.

Yang JH, Maple B, Gao F, Maguire G, Wu SM. Postsynaptic responses of horizontal cells in the tiger salamander retina are mediated by AMPA-preferring receptors. *Brain Research*. 1998 Jun 22;797(1):125-34.

Yazulla S, Kleinschmidt J. Carrier-mediated release of GABA from retinal horizontal cells. *Brain Res*earch. 1983 Mar 14;263(1):63-75.

Zhang AJ, Zhang J, Wu SM. Electrical coupling, receptive fields, and relative rod/cone

inputs of horizontal cells in the tiger salamander retina. *Journal of Comparative Neurology*. 2006 Nov 20;499(3):422-31.

Zhang DQ, Belenky MA, Sollars PJ, Pickard GE, McMahon DG. Melanopsin mediates retrograde visual signaling in the retina. *PLoS One*. 2012;7(8):e42647.

Zhang DQ, Wong KY, Sollars PJ, Berson DM, Pickard GE, McMahon DG. Intraretinal signaling by ganglion cell photoreceptors to dopaminergic amacrine neurons. *The Proceedings of the National Academy of the Sciences in the United States of America*. 2008 Sep 16;105(37):14181-6.

Zhou Y, Bouyer P, Boron WF. Effects of angiotensin II on the CO2 dependence of HCO3- reabsorption by the rabbit S2 renal proximal tubule. American Journal of Physiology. Renal Physiology. 2006 Mar;290(3):F666-73.

Zhou W, Jones SW. The effects of external pH on calcium channel currents in bullfrog sympathetic neurons. *Biophysical Journal*. 1996 Mar;70(3):1326-34.

Reviews

Anastassiou CA, Koch C. Ephaptic coupling to endogenous electric field activity: why bother? *Current Opinion in Neurobiology.* 2015 Apr;31:95-103.

Arshavsky VY, Lamb TD, Pugh EN Jr. G proteins and phototransduction. *Annual Review of Physiology*. 2002;64:153-87.

Baylor DA. Photoreceptor signals and vision. Proctor lecture. *Investigative Ophthalmology & Visual Sciences.* 1987 Jan;28(1):34-49.

Boron WF. Regulation of intracellular pH. *Advances in Physiology Education*. 2004 Dec;28(1-4):160-79.

Burkhardt DA. Synaptic feedback, depolarization, and color opponency in cone photoreceptors. *Visual Neuroscience*. 1993 Nov-Dec;10(6):981-9.

Casey JR, Grinstein S, Orlowski J. Sensors and regulators of intracellular pH. *Nature Reviews Molecular Cell Biology*. 2010 Jan;11(1):50-61.

Chesler M. Regulation and modulation of pH in the brain. *Physiological Reviews*. 2003 Oct;83(4):1183-221.

Euler T, Haverkamp S, Schubert T, Baden T. Retinal bipolar cells: elementary building blocks of vision. *Nature Reviews Neuroscience*. 2014 Aug;15(8):507-19.

Faber DS, Korn H. Electrical field effects: their relevance in central neural networks. *Physiological Reviews*. 1989 Jul;69(3):821-63.

Field GD, Chichilnisky EJ. Information processing in the primate retina: circuitry and coding. *Annual Review of Neuroscience*. 2007;30:1-30.

Imamoto Y, Shichida Y. Cone visual pigments. *Biochimia et Biophysica Acta*. 2014 May;1837(5):664-73.

Jefferys JG. Nonsynaptic modulation of neuronal activity in the brain: electric currents and extracellular ions. *Physiological Review*. 1995 Oct;75(4):689-723.

Kalamkarov G, Pogozheva I, Shevchenko T, Koskelainen A, Hemila S, Donner K. pH changes in frog rods upon manipulation of putative pH-regulating transport mechanisms. *Vision Research*. 1996 Oct;36(19):3029-36.

Luo DG, Xue T, Yau KW. How vision begins: an odyssey. *Proceedings of the National Academy of the Sciences in the United States of America*. 2008 Jul 22;105(29):9855-62.

Masereel B, Pochet L, Laeckmann D. An overview of inhibitors of Na(+)/H(+) exchanger. *European Journal of Medicinal Chemistry*. 2003 Jun;38(6):547-54.

Masland RH. The neuronal organization of the retina. *Neuron*. 2012 Oct 18;76(2):266-80.

Pereda AE. Electrical synapses and their functional interactions with chemical synapses. *Nature Reviews Neuroscience*. 2014 Apr;15(4):250-63.

Piccolino M, Neyton J. The feedback effect from luminosity horizontal cells to cones in the turtle retina: a key to understanding the response properties of the horizontal cells. *Progress in Clinical and Biological Research*. 1982;113:161-79.

Pickard GE, Sollars PJ. Intrinsically photosensitive retinal ganglion cells. *Reviews of Physiology, Biochemistry, and Pharmacology*. 2012;162:59-90

Poudel KR, Bai J. Synaptic vesicle morphology: a case of protein sorting? Curr Opin Cell Biol. 2014 Feb;26:28-33.

Regus-Leidig H, Brandstätter JH. Structure and function of a complex sensory synapse. *Acta Physiologica (Oxford, England)*. 2012 Apr;204(4):479-86.

Rieke F, Baylor DA. Single-photon detection by rod cells of the retina. *Reviews of Modern Physics*.1998 July; 70(3):1027-36.

Rushton WA. Pigments and signals in colour vision. *Journal of Physiology*. 1972 Feb;220(3):1P-P. Review.

Saarikoski J, Ruusuvuori E, Koskelainen A, Donner K. Regulation of intracellular pH in salamander retinal rods. *Journal of Physiology*. 1997 Jan 1;498 (Pt 1):61-72.

Sáez JC, Retamal MA, Basilio D, Bukauskas FF, Bennett MV. Connexin-based gap junction hemichannels: gating mechanisms. *Biochimica et Biophysica Acta*. 2005 Jun 10;1711(2):215-24. Epub 2005 Mar 2. Review.

Schmitz F. The making of synaptic ribbons: how they are built and what they do. *Neuroscientist*. 2009 Dec;15(6):611-24.

Schwartz EA. Transport-Mediated Synapses in the Retina. *Physiological Reviews*. 2002 Jan; 82(4):875-891.

Thoreson WB. Kinetics of synaptic transmission at ribbon synapses of rods and cones. *Molecular Neurobiology*. 2007 Dec;36(3):205-23.

Thoreson WB, Mangel SC. Lateral interactions in the outer retina. *Progress in Retinal and Eye Research*. 2012 Sep;31(5):407-41.

Thoreson WB, Witkovsky P. Glutamate receptors and circuits in the vertebrate retina. *Progress in Retinal and Eye Research*. 1999 Nov;18(6):765-810.

Twig G, Levy H, Perlman I. Color opponency in horizontal cells of the vertebrate retina. *Progress in Retinal and Eye Research*. 2003 Jan;22(1):31-68.

Vaney DI, Sivyer B, Taylor WR. Direction selectivity in the retina: symmetry and asymmetry in structure and function. *Nature Reviews Neuroscience*. 2012 Feb 8;13(3):194-208.

von Békésy G. Mach band type lateral inhibition in different sense organs. *The Journal of General Physiology*. 1967 Jan;50(3):519-32.

Vroman R, Klaassen LJ, Kamermans M. Ephaptic communication in the vertebrate retina. *Frontiers in Human Neuroscience*. 2013 Sep 23;7:612.

Witkovsky P, Stell WK, Ishida AT. Circuits and properties of signal transmission in the retina. *Journal of Neurophysiology*. 2006 Aug;96(2):509-11.

Wright SH. Generation of resting membrane potential. *Advances in Physiology Education*. 2004 Dec;28(1-4):139-42.